

**Title** – Environmental controls on the biogeography of diazotrophy and *Trichodesmium* in the Atlantic Ocean

**Running Title** – Diazotroph biogeography in the Atlantic

**Authors** - Snow J. T.<sup>1</sup>, Schlosser C.<sup>1,2</sup>, Woodward E.M.S.<sup>3</sup>, Mills M.M.<sup>4</sup>, Achterberg E. P.<sup>1,2</sup>, Mahaffey, C.A.<sup>5</sup>, Bibby T.S.<sup>1</sup>, Moore C.M.<sup>1</sup>

<sup>1</sup> Ocean and Earth Science, University of Southampton, National Oceanography Centre, European Way, Southampton, SO14 3ZH, UK

<sup>2</sup> GEOMAR Helmholtz-Zentrum für Ozeanforschung, 24148 Kiel, Germany

<sup>3</sup> Plymouth Marine Laboratory, PL1 3DH, Plymouth, United Kingdom

<sup>4</sup> Biologische Ozeanographie, Forschungsbereich Marine Biogeochemie, Leibniz-Institut für Meereswissenschaften, Dusternbrooker Weg 20, 24105 Kiel, Germany

<sup>5</sup> School of Environmental Sciences, University of Liverpool, Jane Herdman Building, Liverpool L69 3GP, UK

**Corresponding Author:**

**Snow J. T.**

*Email* – j.snow@noc.soton.ac.uk

*Address* - Ocean and Earth Science, University of Southampton, National Oceanography Centre, European Way, Southampton, SO14 3ZH, UK

This article has been accepted for publication and undergone full peer review but has not been through the copyediting, typesetting, pagination and proofreading process which may lead to differences between this version and the Version of Record. Please cite this article as doi: 10.1002/2015GB005090

## Abstract

The cyanobacterium *Trichodesmium* is responsible for a significant proportion of the annual 'new' nitrogen introduced into the global ocean. Despite being arguably the best studied marine diazotroph, the factors controlling the distribution and growth of *Trichodesmium* remain a subject of debate, with sea surface temperature, the partial pressure of CO<sub>2</sub> and nutrients including iron (Fe) and phosphorus (P), all suggested to be important. Synthesising data from 7 cruises collectively spanning large temporal and spatial scales across the Atlantic Ocean, including 2 previously unreported studies crossing the largely under-sampled South Atlantic gyre, we assessed the relationship between proposed environmental drivers and both community N<sub>2</sub> fixation rates and the distribution of *Trichodesmium*. Simple linear regression analysis would suggest no relationship between any of the sampled environmental variables and N<sub>2</sub> fixation rates. However, considering the concentrations of iron and phosphorus together within a simplified resource-ratio framework, illustrated using an idealised numerical model, indicates the combined effects these nutrients have on *Trichodesmium* and broader diazotroph biogeography, alongside the reciprocal maintenance of different biogeographic provinces of the (sub)-tropical Atlantic in states of Fe or P oligotrophy by diazotrophy. The qualitative principles of the resource-ratio framework are argued to be consistent with both the previously described North-South Atlantic contrast in *Trichodesmium* abundance and the presence and consequence of a substantial non-*Trichodesmium* diazotrophic community in the western South Atlantic subtropical gyre. A comprehensive, observation-based explanation of the interactions between *Trichodesmium* and the wider diazotrophic community with iron and phosphorus in the Atlantic Ocean is thus revealed.

### Index Terms:

- 4805 – Biogeochemical cycles, processes, and modelling
- 4840 – Microbiology and microbial ecology
- 4855 – Phytoplankton
- 4845 – Nutrients and Nutrient cycling
- 4875 – Trace elements

### Keywords:

nitrogen fixation, *Trichodesmium*, resource-ratio, nutrient stress, iron, phosphorus

### Key Points:

- Significant diazotrophic community in both north and south Atlantic
- SST and pCO<sub>2</sub> have limited role in diazotroph biogeography of tropical Atlantic
- Combined effects of Fe and P control diazotrophy in (sub)-tropical Atlantic

## Introduction

Nitrogen ( $N_2$ ) fixation by diazotrophs is a crucial component of the global nitrogen cycle and is ultimately responsible for the coupling of the marine nitrogen and phosphorous cycles and the maintenance of oceanic productivity [Falkowski, 1997]. *Trichodesmium*, a colonial, diazotrophic, cyanobacterium has been a major focus of research due to the importance of this organism in influencing the nutrient biogeochemistry of the tropical and subtropical ocean [Sohm *et al.*, 2011b]. With an estimated 22 Tg N yr<sup>-1</sup> fixed by *Trichodesmium* in the North Atlantic alone, this diazotrophic population contributes significantly to annual marine  $N_2$  fixation (~80-200 Tg N yr<sup>-1</sup>) [Capone *et al.*, 2005; Mahaffey *et al.*, 2005; Duce *et al.*, 2008]. However, recent work has emphasised the presence and importance of non-*Trichodesmium* diazotrophy in a range of environments [Moisander *et al.*, 2010; Zehr, 2011]. The balance of different environmental controls on the growth and biogeography of *Trichodesmium*, and diazotrophs in general, remains a matter of debate. Sea surface temperature (SST), pCO<sub>2</sub> and nutrients have all been suggested to be important drivers of diazotrophic activity, growth and hence biogeography [LaRoche and Breitbarth, 2005; Kranz *et al.*, 2009; 2010; Hutchins *et al.*, 2013; Fu *et al.*, 2014]. However, the relative roles of these different drivers on diazotrophy in the modern ocean remain unclear [Luo *et al.*, 2013], significantly limiting our ability to project the future influence of this process on global biogeochemical cycles [Boyd *et al.*, 2010; Moore *et al.*, 2013], or to fully interpret the significant variability in oceanic  $N_2$ -fixation which appears to have occurred in the past [Straub *et al.*, 2013].

Natural populations of *Trichodesmium* are frequently argued to be physiologically constrained to the SST range ~18-34°C, in large part due to correlative abundance observations [LaRoche and Breitbarth, 2005]. However, culture strains of *Trichodesmium* have also been shown to grow optimally at 24-30°C [Breitbarth *et al.*, 2007; Fu *et al.*, 2014]. Other diazotrophs, including heterocystous cyanobacteria, are prevalent in much colder environments, suggesting that elevated temperatures are not a *de facto* prerequisite for diazotrophic growth [Staal *et al.*, 2003; Pandey *et al.*, 2004; Stal, 2009]. Indeed unicellular diazotrophs can be more abundant than *Trichodesmium* at lower temperatures in some regions [Moisander *et al.*, 2010]. Although the evolutionary timescales of temperature adaptation, both in situ and in culture, are largely unknown [Huertas *et al.*, 2011; Thomas *et al.*, 2012], phytoplankton appear to retain temperature optima reflecting that of their isolation environment [Thomas *et al.*, 2012]. Co-variability of temperature with other environmental drivers in oceanic systems, including nutrient availability and water column stratification,

consequently means that direct temperature constraints on diazotroph biogeography, need to be considered alongside the potential for secondary adaptation to conditions found within the realised niche [Monteiro *et al.*, 2011; Dutkiewicz *et al.*, 2012; Ward *et al.*, 2013; Dutkiewicz *et al.*, 2014; Fu *et al.*, 2014].

Numerous *Trichodesmium* isolates and other diazotrophic taxa have been shown to have increased rates of N<sub>2</sub> and CO<sub>2</sub> fixation when cultured at elevated pCO<sub>2</sub> (e.g. current to projected end-of-century levels of ~750-1000 ppm), particularly when compared to preindustrial or Pleistocene glacial pCO<sub>2</sub> concentrations [Barcelos e Ramos *et al.*, 2007; Hutchins *et al.*, 2007; Garcia *et al.*, 2013; Hutchins *et al.*, 2013]. Sensitivities vary between strains [Hutchins *et al.*, 2013], with experimental doubling in pCO<sub>2</sub> typically increasing N<sub>2</sub> fixation rates by 35-100% [Barcelos e Ramos *et al.*, 2007; Hutchins *et al.*, 2007; 2013]. However, similar studies on natural *Trichodesmium* colonies have so far failed to show any such consistent effect [Böttjer *et al.*, 2014; Gradoville *et al.*, 2014]. Current geographical variability in surface water pCO<sub>2</sub> is also substantially less than the projected differences between contemporary ocean and glacial or end of century values [Rödenbeck *et al.*, 2013], suggesting that any pCO<sub>2</sub> sensitivity may be unlikely to exert a significant control on contemporary diazotroph biogeography.

Investigations into the nutritional requirements of *Trichodesmium* and other diazotrophs have focused on the requirements for iron (Fe) and phosphorus (P), with a number of novel nutrient acquisition and utilisation strategies for Fe and P having been described [Dyhrman *et al.*, 2006; Shi *et al.*, 2007; Orchard *et al.*, 2009; 2010; Richier *et al.*, 2012]. *Trichodesmium spp.* are capable of accessing dissolved inorganic phosphorus (DIP) as PO<sub>4</sub><sup>3-</sup> and dissolved organic phosphorus (DOP), in the form of both phosphomonoesters and phosphonates, which may be less widely bioavailable to the general microbial population [Roy *et al.*, 1982; Dyhrman *et al.*, 2006; Sohm *et al.*, 2008; Orchard *et al.*, 2009; 2010]. Recent work has also demonstrated that *Trichodesmium* structural P requirements can be reduced under conditions of low phosphorus availability via replacement of phospholipids for sulpholipids [Van Mooy *et al.*, 2009].

The presence of Fe within nitrogenase is expected to impose an enhanced diazotrophic requirement for this element [Raven, 1988]. In contrast to other diazotrophic cyanobacteria, which can reduce the instantaneous Fe burden through temporal separation of the two iron-rich metabolic processes of CO<sub>2</sub> and N<sub>2</sub> fixation [Saito *et al.*, 2011], *Trichodesmium* fixes both CO<sub>2</sub> and N<sub>2</sub> during the day through a complex combination of temporal and spatial segregation [Berman-Frank *et al.*, 2001; Sandh *et al.*, 2009]. Consequently, Fe requirements

may be further enhanced for *Trichodesmium* as compared to the wider diazotrophic community [Berman-Frank *et al.*, 2007; Richier *et al.*, 2012].

The interface between the North Atlantic Subtropical gyre (NASG) and the South Atlantic Subtropical gyre (SASG) has repeatedly been noted as an environment characterised by high N<sub>2</sub> fixation rates and abundant *Trichodesmium* populations which can dominate the regional diazotrophic community [Tyrrell *et al.*, 2003; Carpenter *et al.*, 2004; Capone *et al.*, 2005; Moore *et al.*, 2009; Großkopf *et al.*, 2012]. Dissolved inorganic nitrogen (DIN) concentrations are persistently low and have been repeatedly demonstrated to proximally limit the abundance and activity of the non-diazotrophic community throughout the low latitude oligotrophic Atlantic [Ryther and Dunstan, 1971; Graziano *et al.*, 1996; Mills *et al.*, 2004; Moore *et al.*, 2009]. In contrast, the concentration of DIP is significantly lower in the NASG when compared to the SASG [Moore *et al.*, 2009], as is evident from the SASG's elevated P\* (where P\* = DIP-DIN/16) [Deutsch *et al.*, 2007]. Similarly, DOP and DOP\* are also elevated in the SASG relative to the NASG [Moore *et al.*, 2009]. In contrast, surface water dissolved iron (DFe) concentrations are higher in the NASG than in the SASG due to atmospheric deposition of iron-rich Saharan dust into the former (Figure 1) [Bowie *et al.*, 2002; Jickells *et al.*, 2005; Conway *et al.*, 2014].

The inter-tropical convergence zone (ITCZ) is a significant contributor to the gradient in atmospheric deposition, shielding the South Atlantic from the high dust air masses of the northern Hemisphere [Schlosser *et al.*, 2014]. Observed high rates of N<sub>2</sub> fixation have been ascribed to the ITCZ and Saharan dust associated supplies of DFe [Moore *et al.*, 2009; Schlosser *et al.*, 2014] (Figure 1), which in turn depletes both DIP and DOP pools of the NASG, subsequently driving P availability down to the point where it may limit further diazotrophic growth [Wu, 2000; Moore *et al.*, 2009]. Consequently, the resupply of DIP, DOP or collectively total dissolved phosphorus (TDP) to the NASG via lateral advection of high P\* and/or DOP<sup>(\*)</sup> water may potentially become the controlling factor on diazotrophy in this system [Mather *et al.*, 2008; Moore *et al.*, 2009; Palter *et al.*, 2010; Straub *et al.*, 2013]. Moreover, the low P availability in the NASG, argued to result from diazotrophy [Wu *et al.* 2000; Moore *et al.* 2009], also results in P stress within the non-diazotroph community [Lomas *et al.*, 2010; McLaughlin *et al.*, 2013] despite N appearing to remain the proximal limiting nutrient [Ryther and Dunstan, 1971; Graziano *et al.*, 1996; Moore *et al.* 2006].

In contrast to high rates of diazotrophy within the inter-gyre transition zone [Moore *et al.*, 2009; Schlosser *et al.*, 2014] and P limitation in the NASG [Wu, 2000; Sañudo-Wilhelmy *et al.*, 2001], reported rates of diazotrophy are typically low within the SASG, presumably as

a result of low Fe availability [Moore *et al.*, 2009; Sohm *et al.*, 2011c]. However, despite the SASG being broadly characterised by higher surface DIP (and hence P\*) than the NASG, a marked region of low surface P\* can be observed on the western side of the southern gyre [Deutsch *et al.*, 2007; Moore *et al.*, 2009]. Moreover, recent observations of H<sub>2</sub> supersaturation have been interpreted to result from significant diazotrophy in this region [Moore *et al.*, 2014].

Understanding extant environmental controls on diazotrophy is particularly important in the context of global change. Changes in SST, pCO<sub>2</sub>, dust-driven iron fertilisation and physical excess P (re)-supply have all been hypothesised to potentially influence rates of N<sub>2</sub> fixation, resulting in possible shifts in the balance between local and global N<sub>2</sub> fixation and denitrification [Falkowski, 1997; Breitbarth *et al.*, 2007; Moore *et al.*, 2009; Hutchins *et al.*, 2013; Straub *et al.*, 2013; Weber and Deutsch, 2014]. The biological processes of N<sub>2</sub> fixation and denitrification, alongside other more minor sources and sinks, must ultimately balance out over sufficiently large time and space scales, in order to prevent the oceanic system from rapidly losing or gaining fixed nitrogen, which would significantly influence oceanic productivity and ultimately atmospheric pCO<sub>2</sub> [Falkowski, 1997; Broecker and Henderson, 1998; Gruber, 2008]. Identifying the scales over which this balance operates and hence establishing the associated timescale and strength of the coupling between the P and N cycles is crucial for understanding the controls on the oceanic N inventory and ultimately the potential for this to alter climate [Falkowski, 1997; Straub *et al.*, 2013; Weber and Deutsch, 2014].

In the current study we assembled a data set of *Trichodesmium* abundances and community N<sub>2</sub> fixation rates measured alongside hypothesised environmental drivers, collected during 7 oceanic cruises using broadly consistent methodologies over the period 2002-2011. Using this comprehensive data set we aim to assess the hypothesised importance of temperature, pCO<sub>2</sub>, Fe and P variability on the distribution of whole community N<sub>2</sub> fixation and *Trichodesmium* in particular. Utilising concepts from resource-ratio theory [Tilman, 1980; Tilman *et al.*, 1982; Ward *et al.*, 2013] our interpretation of observed nutrient (Fe, P) patterns explicitly recognises that limiting nutrient concentrations must reflect the end result of feedbacks within the nutrient-microbial system, rather than being one way drivers of microbial activity [Cullen, 1991; Ward *et al.*, 2013]. The analysed data set thus enabled simultaneous investigation of a full suite of proposed environmental drivers of community diazotrophy and *Trichodesmium* biogeography in a region of pronounced environmental and diazotrophic gradients.



## Methods

### Sampling and hydrography

Sampling was conducted during 7 oceanic cruises: M55 (Oct-Nov 2002, R/V *Meteor*) [Mills *et al.*, 2004], M60 (Mar-Apr 2004, R/V *Meteor*) [Moore *et al.*, 2006; 2008], AMT17 (Oct-Nov 2005, RRS *Discovery*) [Moore *et al.*, 2009], D326 (Jan-Feb 2008, RRS *Discovery*) [Richier *et al.*, 2012], JC32 (Mar-May 2009, RRS *James Cook*), D361 (Feb-Mar 2011, RRS *Discovery*) [Schlosser *et al.*, 2014] and AMT21 (Oct-Nov 2011, RRS *Discovery*) (Figure 1). AMT17, D361 and AMT21 followed a north-south transect approximately along the 25°W meridian, as such data from these 3 cruises will first be considered in a meridional context. M55, M60, D326 and JC32 covered a broader longitudinal area. Data from JC32 and AMT21 were previously unreported, while additional data beyond that already published is presented for D326 and D361.

Precipitation information sourced from the NCEP Reanalysis data provided by NOAA/OAR/ESRL PSD, Boulder, Colorado, USA, (<http://www.esrl.noaa.gov/psd/>) was used as a proxy for the location and seasonality of the ITCZ. We have defined the ITCZ's location during D361 (representative of N. hemisphere Spring), AMT21 and AMT17 (representative of N. hemisphere Autumn) as the area where the surface precipitation flux was  $>2 \times 10^{-5} \text{ Kg m}^{-2} \text{ s}^{-1}$ .

### DIN, DIP, DOP and DFe

During cruises M55, M60, JC32, AMT21 nitrate ( $\text{NO}_3^-$ ), analysed as nitrate + nitrite, nitrite ( $\text{NO}_2^-$ ) and phosphate ( $\text{PO}_4^{3-}$ ) were measured using a Bran and Luebbe AAIII segmented flow, colorimetric, auto-analyser or similar instrument using standard colorimetric techniques [Brewer and Riley, 1965; Grasshoff *et al.*, 1976]. For cruises D326, D361 and AMT17 nanomolar  $\text{NO}_3^-$ ,  $\text{NO}_2^-$  and  $\text{PO}_4^{3-}$  concentrations were determined with standard methods using segmented flow analysis with 2 metre liquid waveguide capillary cells, [Schlosser *et al.*, 2014] for D361 and AMT21 and [Patey *et al.*, 2008] for D326. TDP concentrations were determined during cruises AMT17 [Moore *et al.*, 2009], D326 [Mahaffey *et al.*, 2014] and D361 [Reynolds *et al.*, 2014] by UV oxidation as previously described [Moore *et al.*, 2009; Reynolds *et al.*, 2014]. DOP concentrations were calculated as the difference in phosphate concentration before (DIP) and after (TDP) UV oxidation of seawater samples (i.e.  $\text{DOP} = \text{TDP} - \text{DIP}$ ).

DFe concentrations were determined from surface-water samples collected during M55 [Croot *et al.*, 2004], M60, AMT17 [Moore *et al.*, 2009], D326 [Rijkenberg *et al.*, 2012],

D361 [Schlosser *et al.*, 2014] and AMT21 using a trace-metal clean towed fish or titanium-framed CTD. Samples were filtered using 0.2µm cartridge filters (Acropak/Sartobran P300 or similar) and acidified with ultra-clean grade HCl (UpA Romil) to pH1.9 (~0.013 mol H<sup>+</sup> L<sup>-1</sup>). Samples from D361 were analysed using a flow injection analysis (FIA) system equipped with a Toyopearl AF-Chelate-M650 (Tosch) resin via luminol chemiluminescence [Klunder *et al.*, 2011]. Surface seawater samples collected during AMT21 were analysed for Fe by off-line isotope dilution inductively coupled plasma – mass spectrometry (ID-ICP-MS) (Element XR, Thermo), following previously outlined methods [Milne *et al.*, 2010]. The accuracy of previously unreported AMT21 data was assessed by the determination of Fe in seawater reference materials (SAFe and GEOTRACES). The standard seawaters were in good agreement with the reported consensus values (GD = 0.940 nmol L<sup>-1</sup> (1.00 nmol L<sup>-1</sup>), SAFe S = 0.095 nmol L<sup>-1</sup> (0.093 nmol L<sup>-1</sup>), SAFe D2 = 0.933 nmol L<sup>-1</sup> (0.933 nmol L<sup>-1</sup>)).

### **pCO<sub>2</sub> and SST**

Near surface temperature (~2 m, henceforth assumed to be SST) was measured throughout all 7 cruises using a vessel mounted Seabird 38 or similar temperature sensor. For cruises, AMT21, AMT17, D326, M55 and M60 direct measurement of pCO<sub>2</sub> were conducted as described in [Hardman-Mountford *et al.*, 2008], [Kitidis *et al.*, 2012] and [Körtzinger, 1999]. During D361 and JC32 dissolved inorganic carbon (DIC) and total alkalinity (TA) was sampled from near-surface fired Ocean Test Equipment (OTE) bottles. DIC analysis was performed using the standard coulometric technique whilst TA was analysed using standard titrimetric techniques [Dickson *et al.*, 2007]. The partial pressure of CO<sub>2</sub> was derived from these parameters following equations outlined in [Dickson *et al.*, 2007].

### ***Trichodesmium* sp. abundance**

*Trichodesmium* abundance was measured during AMT17, JC32, D326, D361 and AMT21. Entire 20 L OTE bottles fired near the surface (~2 m) were gravity filtered through membranes or polycarbonate filters (Millipore Isopore, 10 µm pore size, 47 mm diameter). Colonies and free trichomes were gently agitated to remove them from the surface of the membrane or filter before being preserved in 2% Lugol's iodide and stored in the dark. Filters were visually inspected for complete re-suspension of *Trichodesmium* colonies and free trichomes. Colony and free trichome abundance, colony morphology and approximate colony size were enumerated using light microscopy. The limit of detection for *Trichodesmium* abundance was equivalent to 0.05 Trichomes L<sup>-1</sup>.



## N<sub>2</sub> Fixation Rates

Whole community N<sub>2</sub> fixation rates were measured during M55, M60, AMT17, JC32, D326, D361 and AMT21 following the method described by [Montoya *et al.*, 1996]. Briefly, 4.5 L (AMT17, D326, D361 JC32 and AMT21) or 1.2 L (M55 and M60) polycarbonate bottles (Nalgene) were filled, ensuring no air bubbles remained and sealed with silicone septa containing screw-caps. Each bottle was spiked with 4 ml (AMT17, D326, D361 JC32 and AMT21) or 1 ml (M55 and M60) <sup>15</sup>N<sub>2</sub> gas (99%, Campro or Cambridge Scientific, see below) and incubated for 24 hours at sea surface temperature (SST) and near sea surface irradiance (SSI) achieved using on deck incubators cooled using the ship's underway seawater supply system and shaded using optical filters (0.15 neutral density). Following incubation samples were filtered onto pre-ashed glass-fibre filters (450°C for 12 hours, Whatman GF/F or Fisherbrand MF300), folded into 1.5 ml tubes (Eppendorf) and dried for 24 hours at 40°C. Upon return to the lab filters were encapsulated in a tin disc and analysed for organic nitrogen and <sup>15</sup>N/<sup>14</sup>N ratio using Elemental Analyser Isotope Ratio Mass Spectrometry.

*Trichodesmium* specific N<sub>2</sub> fixation rates were also measured during both D361 and AMT21. Colonies were collected at dawn using plankton net tows. 50 colonies were then isolated using plastic inoculation loops and placed into 125 ml polycarbonate bottles (Nalgene) filled with 0.22 µm filtered trace-metal clean surface water. Bottles were filled entirely, sealed with silicone septa containing screw caps and spiked with 0.5 ml <sup>15</sup>N<sub>2</sub>. Bottles were incubated for 12 hours at SST and sea surface irradiance before being filtered onto pre-ashed GF/F filters, dried and stored until analysis according to the method described for the whole community.

Recent work has highlighted potential contamination issues with commercial <sup>15</sup>N<sub>2</sub> gas stocks [Dabundo *et al.*, 2014]. The stocks used during the reported cruises were purchased from Campro Scientific (M55 and M60, lot numbers not recorded) and Cambridge Isotopes (AMT17, D326 - lot # I1-8518; JC32, D361, AMT21 - lot # I1-11785A). Although these stocks are either known (Cambridge Isotopes lot # I1-11785A), or were likely to be relatively clean [Dabundo *et al.*, 2014], using a similar calculation to [Dabundo *et al.*, 2014] we estimated a potential upper bound for apparent N<sub>2</sub> fixation due to contaminants (i.e. an effective detection limit) of ~0.05 nmol N m<sup>-2</sup> d<sup>-1</sup>. Additionally a systematic ~2 fold underestimation of the absolute N<sub>2</sub> fixation rates is likely to have influenced the absolute rates derived due to incomplete equilibration of the N<sub>2</sub> gas over the experimental timescale [Mohr *et al.*, 2010; Großkopf *et al.*, 2012; Wilson *et al.*, 2012]. However, given that observed

community rates and *Trichodesmium* specific rates spanned >2 and >3 orders of magnitude respectively, neither background apparent rates due to gas contamination or systematic underestimation are likely to have any significant bearing on our conclusions, which are based on the observed interrelationship between variables within the data set.

### **Numerical Model**

To support our observations and the conceptual resource ratio framework used for interpreting the nutrient-diazotroph interrelationships, we used a previously employed numerical box model [Tyrrell, 1999; Dutkiewicz *et al.*, 2012; Ward *et al.*, 2013; Schlosser *et al.*, 2014]. The differential equations describing the evolution of state variables were effectively identical to those detailed in [Ward *et al.*, 2013] and [Schlosser *et al.*, 2014], with parameters, model equations and initial conditions as described in the latter. Briefly, the model is integrated in a series of linked boxes taken to represent the ‘surface’ and ‘thermocline’ regions of the water column. Three nutrients (N, P and Fe) interact with diazotrophs and non-diazotrophs in the surface boxes, while organic material transported to the ‘thermocline’ box is simply remineralised back to dissolved nutrients [Schlosser *et al.*, 2014]. The model was further expanded to include two distinct diazotrophs (D1 and D2), with D1 parameterised as in [Schlosser *et al.*, 2014] whilst D2 was ascribed a 20% elevated P requirement alongside a 20% reduction in Fe requirement, making it a better competitor for P but a poorer competitor for Fe. The only external forcing provided is a variable source of DFe to one or more of the surface boxes, which was originally taken to represent differing atmospheric Fe input scenarios [Schlosser *et al.*, 2014], although this could be equally applicable to any other Fe sources including for example, riverine or sedimentary inputs. For the current study, iron input was arbitrarily represented by a Gaussian distribution with a half width of 4 surface boxes and peak inputs that were varied over a twenty fold range between 28 runs.

### **Results and Discussion**

Sea surface temperatures ranged from 19.6 - 28.7 °C, with a single station (JC32) located in the upwelling region to the west of Africa having a lower temperature of 16.4 °C (23.7 °S, 13.7 °E). Excepting this station, all observed temperatures were within previously published temperature tolerances (18-32 °C) for a range of *Trichodesmium* culture strains [LaRoche and Breitbarth, 2005; Breitbarth *et al.*, 2007; Fu *et al.*, 2014] and temperature ranges observed to be associated with other groups [Moisander *et al.*, 2010]. Observed variability in pCO<sub>2</sub> across the sampled region was modest (332 - 464 µatm), with absolute values typically higher than

half saturation constants ( $K_{1/2}$ ) for  $N_2$  fixation as a function of  $pCO_2$  for the majority of studied *Trichodesmium* culture strains [Hutchins *et al.*, 2013].

The location of the ITCZ is affected by sea surface temperature (SST) and as such the ITCZ shows an asymmetrical seasonal migration [Mitchell and Wallace, 1992] which influences the position of the biogeochemical transition region between the northern and southern oligotrophic regions of the Atlantic [Schlosser *et al.*, 2014]. The seasonal synchronicity between precipitation and DFe distributions in the (sub)-tropical Atlantic as described in [Schlosser *et al.*, 2014] is further supported in the current study with the inclusions of the previously unpublished  $N_2$  fixation data from AMT21 (Figure 2E). The region of maximal precipitation, used here to represent the location of the ITCZ, was observed between 4 °N and 8 °S during D361, whilst for AMT21 & AMT17 maximum precipitation was observed further north between 11.5°N - 2°N and 10.5°N - 4°S respectively (Figure 2). The ITCZ is at its northern and southern most position in July and January respectively [Philander *et al.*, 1996; Xie and Saito, 2001]. Given the dates of D361 and AMT21/AMT17 are mid-phase in relation to this seasonality, it is likely that there is a greater latitudinal migration than our observations indicate.

Surface DIN concentrations remained consistently low throughout the sampled regions, with a mean concentration of  $12 \pm 10$  nM (mean  $\pm$  SD,  $n = 276$ ) (Figure 2A and 4A,E & I). The NASG consistently displayed greatly diminished DIP concentrations when compared with the SASG ( $22 \pm 19$  nM ( $n = 126$ ) and  $126 \pm 60$  nM ( $n = 197$ ) respectively) (Figures 2B, 3A and 4B, F & J). Conversely the distribution of DFe revealed consistently elevated concentrations in the Saharan-dust influenced NASG ( $0.42 \pm 0.33$  nM,  $n = 189$ ) when compared with the SASG ( $0.13 \pm 0.11$  nM,  $n = 107$ ) where little dust-deposition is evident [Jickells, 2006] (Figure 2C, 3B). The new measurements from the AMT21 cruise presented here were consistent with prior analysis based on the D361 and AMT17 cruises [Schlosser *et al.*, 2014], suggesting that observed north-south migration of DIP and DFe gradients is associated with the seasonal migration of the ITCZ [Schlosser *et al.*, 2014]. Specifically, AMT 21 and 17 showed elevated DFe concentrations in the central NASG around 20 - 5 °N whilst D361 (red) shows this band of high DFe shifted south between 5 °N and 0 °N (Figure 2C and 3B).

*Trichodesmium* colonies and free trichomes were observed during all 7 cruises. Near-surface *Trichodesmium* abundance was densest in the southern region of the NASG and seasonally associated with the ITCZ influenced region (~15 °N - 7 °S) (Figure 2D and 3D), consistent with previous observations [Capone *et al.*, 2005; Fernandez *et al.*, 2010; Sohm *et*

*al.*, 2011b; Luo *et al.*, 2012; Schlosser *et al.*, 2014]. Observations from AMT21 & AMT17 revealed *Trichodesmium* to be consistently abundant throughout the sampled regions of the NASG (mean  $\pm$  SD,  $76 \pm 33$  and  $\sim 70 \pm 64$  trichomes  $L^{-1}$  respectively) before sharply declining to undetectable concentrations south of  $\sim 0^\circ N$ . The observed population density maximum during D361 was located further south, with *Trichodesmium* observed between  $19^\circ N$  and  $\sim 7^\circ S$  ( $82 \pm 72$  trichomes  $L^{-1}$ ) (Figure 2D). Consistent with previous observations [Moore *et al.*, 2009; Sohm *et al.*, 2011a], *Trichodesmium* was not observed in the central SASG during any of these cruises. In contrast, during the JC32 cruise, significant *Trichodesmium* populations and associated community  $N_2$  fixation rates were observed within the core of the Brazil current, adjacent to the continental shelf on the far western edge of the SASG. On-shelf blooms of *Trichodesmium* have also been reported in this region [Carvalho *et al.*, 2008]. Moreover, enhanced rates of community  $N_2$  fixation were directly observed in the upper water column during the north-southwest crossing of the western side of the SASG during AMT21 (Figure 4D).

Surface community  $N_2$  fixation rates observed across large regions of the Atlantic correlated well with *Trichodesmium* biomass ( $r = 0.72$ ,  $P < 0.05$ ) particularly over the range of higher  $N_2$  fixation rates and *Trichodesmium* abundances (Figure 5). At lower *Trichodesmium* abundance the observed relationship decouples, likely representing an increased contribution of the non-*Trichodesmium* diazotrophic community to measured whole-community  $N_2$  fixation rates, potentially alongside any contribution by trace level contaminants in  $^{15}N_2$  gas [Dabundo *et al.*, 2014]. Mean *Trichodesmium* specific  $N_2$  fixation rates assessed during both D361 and AMT21 ( $n = 24$ ) supported the inferred increased contribution of the non-*Trichodesmium* diazotrophic community at lower  $N_2$  fixation rates, although any potential for differential underestimation of  $N_2$  fixation rates between diazotrophic groups [Großkopf *et al.*, 2012] could weaken such inferences. Acknowledging such caveats, elevated whole community  $N_2$  fixation appeared a strong indicator of *Trichodesmium* specific  $N_2$  fixation, in agreement with previous work [Fernandez *et al.*, 2010] in the tropical Atlantic, where observed  $N_2$  fixation rates closely matched predicted  $N_2$  fixation rates derived from *Trichodesmium* abundance.

Surface community  $N_2$  fixation rates showed a similar north-south divide as observed in *Trichodesmium* abundance, with the bulk of diazotrophic activity observed in the southern flanks of the NASG and the equatorial region (Figure 3C and 6A & B) consistent with previous observations [Luo *et al.*, 2012]. Within the boundary between the NASG and SASG, a strong seasonality is observed between spring (D361, red) and autumn (AMT17, blue &

AMT21, green) cruises where peak surface N<sub>2</sub> fixation rates follow the pattern of DFe and reside further south during D361 when compared with either AMT cruise (Figure 2) as previously indicated [Schlosser *et al.*, 2014].

### Simple Linear Regression Analysis

Relationships between environmental and diazotroph related variables were initially investigated using simple linear regression analysis as in [Luo *et al.*, 2013]. A weak ( $R^2 < 0.07$ ) yet significant negative correlation was observed between surface N<sub>2</sub> fixation and DIP (Figure 7C and Table 1). No other significant correlation was found between SST, pCO<sub>2</sub> DIP or DFe and *Trichodesmium* abundance or SST, pCO<sub>2</sub> or DFe and surface N<sub>2</sub> fixation rates (Figure 7 and Table 1). Variations in these 4 environmental variables, all of which have been proposed as potential controls on diazotrophy, were thus of limited predictive value for measured community N<sub>2</sub> fixation rates or *Trichodesmium* biogeography across the observed environmental ranges in the (sub)-tropical Atlantic (Figure 7).

As noted above, the sampled range for SST was within the temperature tolerance range of studied *Trichodesmium* isolates [Fu *et al.*, 2014]. Moreover, the current analysis contrasts with the findings of [Luo *et al.*, 2013] who observed a significant correlation between temperature and N<sub>2</sub> fixation across a broader temperature and geographical range. Overall, it is clearly difficult to establish any strong inference from within correlative studies of this type. Thus it remains unclear whether large scale correlations of SST and *Trichodesmium* populations provide evidence for the importance of a direct physiological driver [Fu *et al.*, 2014], or result from stronger control by co-varying factors such as low N environments and increased stratification, with temperature optima then being a secondary adaptation [LaRoche and Breitbarth, 2005; Ward *et al.*, 2013]. Irrespectively, within the sampled range, any direct temperature related ecophysiological effect [Fu *et al.*, 2014] appears to be overridden by other drivers.

On the basis of the performed correlation analysis, the marked coherent order of magnitude variability we observed in overall diazotrophy and *Trichodesmium* abundance also appeared to be unrelated to any direct physiological pCO<sub>2</sub> driver. Although observed pCO<sub>2</sub> values in the sampled region were typically higher than most measured *Trichodesmium* K<sub>1/2,pCO2</sub> (Fig 7b), some currently studied strains have higher values [Hutchins *et al.*, 2013]. Thus the potential for pCO<sub>2</sub> to have a selective influence between *Trichodesmium* ecotypes can certainly not be excluded on the basis of our observations, but once again, any effect on



the overall biogeography of *Trichodesmium* or the bulk diazotroph community appeared to be overridden, or at least masked, by other factors.

The absence of predictive capability for DIP and DFe as individual variables contrasts with a prior analysis based on a subset of this data [Moore *et al.*, 2009], but is more consistent with the broader study of [Luo *et al.*, 2013]. However, unlike SST and pCO<sub>2</sub>, which will not be directly influenced by the activity of diazotrophs, or, in the case of pCO<sub>2</sub> only weakly influenced at most [Foster *et al.*, 2007; Subramaniam *et al.*, 2008], reciprocal feedbacks between microbial processes and any nutrients potentially limiting these processes are expected to be strong, to the point of potentially being dominant controls [Tilman, 1980; Cullen, 1991; Ward *et al.*, 2013]. The lack of a direct correlation between a limiting nutrient and organism biogeography or activity would be fully expected under many circumstances [Cullen, 1991] and certainly cannot provide unequivocal evidence for the absence of a relationship. Indeed, if it is assumed that both DIP and DFe are essential nutrients sensu [Tilman, 1980], with diazotrophs in general and *Trichodesmium* in particular requiring both for growth, relationships between both these nutrients and N<sub>2</sub> fixation and/or *Trichodesmium* abundance must all be considered together within a theoretical framework capable of explaining observations [Dutkiewicz *et al.*, 2012; Ward *et al.*, 2013; Dutkiewicz *et al.*, 2014].

### **Resource-ratio Theory**

Resource competition theory dictates that the organism best able to utilise a given resource will deplete that resource down to a well defined minimum concentration, termed the R\* value [Tilman, 1980]. At steady state this framework supports a niche for as many competing species as there are different potential limiting resources. Temporarily considering nutrients as the sole potential limiting resource, the abundance and activity of the diazotrophic community is expected to be controlled by the relative supply rates of N, P and Fe [Ward *et al.*, 2013]. Diazotrophs such as *Trichodesmium* will avoid competitive exclusion by non-diazotrophs in regions where the non-diazotrophic community is N limited [Monteiro *et al.*, 2011; Dutkiewicz *et al.*, 2012; Ward *et al.*, 2013]. Such steady state N limitation of non-diazotrophs is likely a reasonable approximation for the sampled regions of the (sub)-tropical Atlantic [Moore *et al.*, 2013], consistent with the observed uniform low (<20nM) DIN concentrations (Figure 2A) and multiple experimental studies [Ryther and Dunstan, 1971; Graziano *et al.*, 1996; Mills *et al.*, 2004; Moore *et al.*, 2009].

Adopting the simplest assumption, where diazotrophs consume Fe and P at a fixed ratio, as net growth proceeds from a starting condition, both nutrients would be expected to be



removed along a fixed consumption vector (Figure 8A) until one is depleted to the  $R^*$  concentration [Ward *et al.*, 2013]. Once a nutrient has been depleted to  $R^*$ , equilibrium uptake is balanced by supply and zero net growth is achievable. Under this condition the biomass of the stable diazotroph population will then be proportional to the (re)-supply of the limiting nutrient divided by the mortality rate [Dutkiewicz *et al.*, 2009; 2012], i.e. the diazotroph standing stock and overall diazotrophy is not expected to be related to the steady state concentration of the limiting nutrient. Consequently, over a sufficiently large range of Fe or P supply ratios, the interaction between diazotrophic growth and Fe and P availability is expected to result in a characteristic ‘L-shaped’ relationship between the residual Fe and P concentrations at equilibrium (Figure 8A). The corner of the ‘L’, which represents the optimal Fe:P supply ratio, defines the transition between either Fe or P limitation, with populations of diazotrophs located along the  $R_{Fe}^*$  isocline being Fe limited, while populations along the  $R_P^*$  isocline are P limited (as illustrated in Figure 8A).

Such conceptual arguments can be illustrated using simple numerical models of the system [Dutkiewicz *et al.*, 2012; Ward *et al.*, 2013; Schlosser *et al.*, 2014]. Crucially, the magnitude of the equilibrium diazotroph biomass is expected to depend on the absolute supply rates of the limiting nutrient and mortality [Dutkiewicz *et al.*, 2012; Ward *et al.*, 2013], while the nutrient limitation status is entirely dictated by the supply ratios of different nutrients compared to biological requirements [Ward *et al.*, 2013]. Thus, even within a simple illustrative numerical model, where the activity and abundance of diazotrophs is entirely controlled by parameterised nutrient limitation, there is no simple equilibrium relationship between diazotrophic activity or biomass and the concentration of either nutrient (Figure 8B), emphasising how observed concentrations of limiting nutrients are expected to be a consequence of microbe-nutrient interactions [Cullen, 1991; Ward *et al.*, 2013]. In contrast, within the current context, a robust, repeatable characteristic L-shaped relationship between two limiting nutrients, P and Fe, emerges as a result of diazotrophic activity (Figure 8B). The arms of the ‘L’ reflect the so called zero-net growth isoclines [Tilman *et al.*, 1982] corresponding to the  $R^*$  values for the respective nutrients (Figure 8), which in the simplest case are given by [Tilman, 1980; Dutkiewicz *et al.*, 2012; Ward *et al.*, 2013]:

$$R_{Fe}^* = \frac{k_{Fe}}{\frac{\mu_{max}}{m}} \quad \text{Eq. 1}$$

$$R_p^* \frac{k_p}{\frac{\mu_{\max}}{m}} \quad \text{Eq. 2}$$

Where  $k_{\text{Fe}}$  and  $k_{\text{P}}$  represent the half saturation coefficients for growth on Fe and P respectively and  $\mu_{\max}$  and  $m$  are the maximum growth rate and total mortality rate respectively.

Within the adopted framework for the model [Schlosser *et al.*, 2014], peak diazotroph biomass within a single realisation occurs strictly at the apex of the ‘L’. However, performing multiple runs, for example varying the magnitude of peak Fe input, can reveal more complex emergent patterns of diazotrophy. Although there is a tendency for the highest biomass to typically occur around the low Fe – low P transition region (Figure 8B), high rates can actually be found along the arms of the ‘L’ as, to reiterate again, biomass and activity are a function of both limiting nutrient supply rate and mortality, while the equilibrium limiting nutrient concentration is independent of supply [Dutkiewicz *et al.*, 2009; 2012; Ward *et al.*, 2013].

Comparing our compiled data set with these simple conceptual and numerical models (Figure 8A & B), we observed a characteristic L-shaped relationship between residual surface DIP and DFe concentrations in the sampled regions of the oligotrophic Atlantic Ocean (Figure 9A & C). Moreover, despite less data being available, a similar relationship was observed between TDP and DFe (Figure 9B & D). Similarly, incorporation of a range of treatments of DOP and DON cycling within the model framework (not shown), introduced no qualitative difference in the emergent relationships between DFe and DIP\* and TDP\* compared to the simplest case (Figure 8).

Community  $\text{N}_2$  fixation and *Trichodesmium* abundance both displayed a tendency towards maximal values in regions observed to be depleted in both DFe and DIP (TDP), i.e. generally associated with the transition between regions of higher residual DFe and DIP (Figure 9). We thus suggest that recognition of the potential for diazotrophic activity to drive depletion of DIP (TDP) and/or DFe, as would be predicted from theory [Ward *et al.*, 2013] and occurs within the simple model (Figure 8), in keeping with more complex realisations [Monteiro *et al.*, 2011; Dutkiewicz *et al.*, 2014], is crucial for interpreting observed relationships between diazotrophs and these potentially limiting nutrients in the ocean (Figures 7 & 10). Recent evidence has also suggested that diazotrophs may have a preference for simultaneous DFe and DIP depleted regions [Garcia *et al.*, 2015]. However it is not clear

how such behaviour would influence the large-scale patterns between DFe and DIP observed in the Atlantic (Figure 9).

The observed L-shaped relationship between DIP and DFe is thus argued to be both a result of, and diagnostic of, large scale controls and feedbacks between limiting nutrients and diazotrophy over our sampled region, with ambient DFe and DIP concentrations residing at, or close to, their  $R^*$  concentrations, whilst overall community  $N_2$  fixation rates and/or the standing stock of *Trichodesmium* are then a function of the Fe or P supply rate, rather than the concentrations of these nutrients. The conformity of our environmental observations to the theoretical expectations strongly supports an argument for persistent contrasting regions of Fe and P limitation [Moore et al., 2009; Sohm et al., 2011b] characterising the sampled region of the Atlantic ocean, whilst at the same time questioning the proximal importance of other proposed drivers such as SST and  $pCO_2$  [Breitbarth et al., 2007; Hutchins et al., 2013], at least within the (sub)-tropical Atlantic Ocean.

### **Diazotrophy in the western SASG**

In addition to the *Trichodesmium* attributed diazotrophic activity of the NASG and equatorial Atlantic, our observations revealed significant rates of  $N_2$  fixation in the western-SASG (Figure 3C and 4D). The SASG is grossly under sampled with regards to  $N_2$  fixation rates, with few published data, the majority being surface-water only [Luo et al., 2012]. Comparing the NASG and SASG along the AMT21 transect which sampled the western side of the gyre we calculated near equivalent basin average areal rates between the two gyres with  $\sim 1.1$  and  $\sim 0.90$  mol N  $m^{-2} d^{-1}$  fixed in the NASG and SASG leg of this transect respectively (Figure 6A). Similarly, depth integrated rates during the JC32 west-east transect across the gyre peaked near to the western margin in a region of depleted DIP, low surface  $P^*$  and low  $\delta^{15}N$  approaching 0 per mil (Figure 6B & D). The latter is also consistent with an increased importance for  $N_2$  fixation [Montoya et al., 2004; Mahaffey et al., 2005] in the western SASG as opposed to the eastern basin. Recent observations of  $H_2$  supersaturation are also suggestive of a significant diazotrophic community in the western portion of the SASG basin [Moore et al., 2014] and are consistent with our new direct, and likely underestimated [Mohr et al., 2010; Großkopf et al., 2012; Wilson et al., 2012] observations of significant  $N_2$  fixation the region.

As has been previously observed [Carpenter et al., 2004; Capone et al., 2005], highest rates of diazotrophy in the NASG are typically observed in near surface waters (Figure 4D). In contrast our observation of SASG diazotrophy indicated a more

homogeneous distribution throughout the entire euphotic zone (Figure 4D). Unicellular diazotrophs often appear to be more homogeneously distributed throughout the euphotic zone when compared with *Trichodesmium* [Montoya et al., 2004], which can tend to aggregate in surface waters, but has rarely been observed in the SASG [Tyrrell et al., 2003; Moore et al., 2009; Fernandez et al., 2010; Goebel et al., 2010]. We thus suggest that emerging consistent evidence of significant diazotrophic activity in the western SASG is potentially associated with unicellular diazotrophs, which may be heterotrophic or cyanobacterial in origin and irrespectively might be expected to have different nutrient affinities or growth strategies.

In contrast to the NASG, where high rates of *Trichodesmium* associated N<sub>2</sub> fixation have a tendency to be distributed along the R\*<sub>P</sub> 'arm' of the 'L-shaped' DFe – P relationship (Figure 9A), the SASG diazotrophic community is associated with the R\*<sub>Fe</sub> arm, where DFe concentrations are low (Figure 9A). Higher Fe requirements for *Trichodesmium* as a result of near concurrent N<sub>2</sub> fixation and photosynthetic activity [Berman-Frank et al., 2001], might be expected to result in competitive exclusion by any hypothesised unicellular diazotrophic community under conditions which are Fe limiting for diazotrophy [Monteiro et al., 2010]. For example, the unicellular diazotroph *Crocospheara watsonii* employs a mechanism of iron 'hot-bunking' whereby temporal segregation of N<sub>2</sub> fixation and photosynthesis allows for an intracellular recycling of metalloprotein bound iron [Saito et al., 2011] thus reducing the effective R\*<sub>Fe</sub>. Such an iron-conservation strategy is unlikely in *Trichodesmium* given the substantially shorter time period between peak N<sub>2</sub> fixation and photosynthesis [Berman-Frank et al., 2001]

Dominance of *Trichodesmium* within the 'high Fe-low P' NASG but not the 'lower Fe-higher P' SASG could thus be interpreted as indicating that *Trichodesmium spp.* are the best diazotrophic competitors for P (i.e. have a lower R\*<sub>P</sub>). *Trichodesmium spp.* appear to have a number of novel P compensatory adaptations, including the potential for uptake of a wide range of DOP compounds [Dyhrman et al., 2006; Orchard et al., 2009; 2010], which is broadly consistent with observed depletion of DOP in the NASG [Moore et al., 2009]. Indeed, organisms access the phosphomonoester proportion of the DOP pool using the exoenzyme alkaline phosphatase, with the activity of these enzymes appearing to be maximal when SRP concentrations are around 10-50 nM [Lomas et al., 2010; Wurl et al., 2013; Mahaffey et al., 2014]. Within the NASG, relative to the bulk community, *Trichodesmium* appears to be a better competitor for phosphomonoesters than for DIP [Orchard et al., 2010].

Differences in mortality might also be expected to influence R\* (Eq. 1 & 2). Thus, for example, any reduced grazing pressure on the colonial *Trichodesmium* relative to

competing unicellular diazotrophs would have a tendency to lower both  $R_P^*$  and  $R_{Fe}^*$  for the former (Eq. 1 and Eq.2). Considering competition between *Trichodesmium* and unicellular diazotrophs from this perspective it is thus interesting to speculate whether lowered mortality could contribute to *Trichodesmium* having a lower  $R_P^*$  and hence being the better competitor for P, while higher overall Fe requirements for *Trichodesmium* [Berman-Frank *et al.*, 2007] may be insufficient to offset any lowered mortality in the case of  $R_{Fe}^*$  leaving unicellular diazotrophs as better competitors for Fe.

Potential differences in relative mortality rates, Fe requirements, P requirements and P uptake mechanisms could hence all be argued to result in *Trichodesmium* being the best diazotrophic competitor for P (lowest  $R_P^*$ ) while unicellular diazotrophs are better competitors for Fe (lower  $R_{Fe}^*$ ). Dominance of *Trichodesmium* in the low P-high Fe regime of the NASG (Figure 9A) and non-*Trichodesmium* diazotrophs in the SASG would be consistent with such suggestions. Consistent with previous work [Monteiro *et al.*, 2010], modification of the simple numerical model to include two diazotrophs illustrates these arguments (Figure 10). Specifically, the simple model extension results in dominance of a putative *Trichodesmium* type diazotroph along the  $R_P^*$  arm, with a putative non-*Trichodesmium* type along the  $R_{Fe}^*$  arm (Figure 10), when the former are assumed to be the better P competitor and poorer Fe competitor. In this regard the western-SASG may be analogous to the Pacific Ocean, where  $P^*$  values are elevated and DFe concentrations may be reduced [Martino *et al.*, 2014] creating an environment where unicellular diazotrophs are often able to out-compete *Trichodesmium* for the available Fe [Monteiro *et al.*, 2010].

More generally, both taxonomic and stoichiometric diversity within natural systems would in reality tend to result in multiple  $R^*$  values representing a diverse and complex diazotroph community [Monteiro *et al.*, 2010]. Moreover, away from the dominant large atmospheric sources of dust from North Africa [Conway *et al.*, 2014], other Fe inputs including sedimentary [Moore and Braucher, 2008] and hydrothermal [Saito *et al.*, 2013] may need to be considered. For example, the argued depletion of  $P^*$  due to significant diazotrophy in the western South Atlantic gyre (Figure 4C & 4D), may result from a combination of Patagonian dust inputs or sedimentary inputs from the eastern South American shelf. However, the emergent qualitative relationships we highlight between limiting nutrients are generally expected to be robust to complexities including diversity of Fe source, diazotroph community and stoichiometric variability [Monteiro *et al.*, 2010; Ward *et al.*, 2013].

## Implications for scales of N-P coupling

In order to prevent large swings in oceanic productivity, feedback mechanisms are assumed to couple the N and P cycles over sufficiently large time and space scales [Falkowski, 1997; Tyrrell, 1999]. The scales over which this coupling operates are a crucial determinant of potential variability in the oceanic N inventory and are likely dictated by the significance of any environmental drivers of diazotrophy beyond the supply of excess P [Codispoti, 2007; Deutsch et al., 2007; Moore et al., 2009; Weber and Deutsch, 2014]. Our compiled observational data set indicating significant diazotrophy within both the NASG and SASG (Figures 2C, 3E, 4 and 5A & B), alongside the presence of at least some areas of depleted P (~zero P\*) in both gyres (Figures 2A and 4C & K), is consistent with the dominance of regional scale coupling indicated by recent data constrained modelling [Weber and Deutsch, 2014]. However, observed relationships between DFe, DIP (alongside DOP and TDP) and patterns of diazotrophy also suggests significant local-regional scale controls on diazotrophy beyond excess P supply alone (Figure 9). Moreover, a degree of decoupling between local fixed N loss and N<sub>2</sub> fixation is apparent in the Atlantic, particularly in the NASG, where external inputs of P\* appear to be required to sustain diazotrophy [Moore et al., 2009; Palter et al., 2010]. Although the estimated extent of decoupling in the Atlantic is minor in global terms, being <15% of the global fixed N budget [Moore et al., 2009], the observed high rates of diazotrophy in the southern region of the NASG remain indicative of some degree of decoupling at local through to basin scales, as is likely necessary in order to prevent strong positive feedbacks on fixed N loss in oceanic oxygen minimum zones [Canfield, 2006; Landolfi et al., 2013].

As suggested by a range of modelling studies [Monteiro et al., 2011; Dutkiewicz et al., 2012; Ward et al., 2013; Dutkiewicz et al., 2014], dual Fe-P control on diazotrophy [Falkowski, 1997; Wu, 2000; Moore et al., 2009; Schlosser et al., 2014], as further supported by the current study (Figure 2 and 9), generates the potential for altered patterns of N<sub>2</sub> fixation under a range of global change scenarios. For example, within the regions of significant excess P\* in the low Fe eastern SASG, altered patterns or even magnitudes of diazotrophy might be expected under altered Fe or macronutrient inputs [Dutkiewicz et al., 2014]. Moreover, given the potential importance of southern sourced mode/intermediate waters for P\* supply to the north [Moore et al., 2009; Palter et al., 2010; Straub et al., 2013], any hypothetical alterations to diazotrophy in the SASG might be expected to result in opposite and potentially compensatory changes in N<sub>2</sub> fixation within the NASG. The potential for multiple environmental controls (e.g. P, Fe, temperature, pCO<sub>2</sub>) on diazotrophs,



as indicated here (Figures 7 and 9) and further suggested by culture studies [Breitbarth *et al.*, 2007; Hutchins *et al.*, 2007; 2013; Fu *et al.*, 2014], thus requires that patterns of N<sub>2</sub> fixation and diazotroph biogeography, alongside the potential for these to change, be interpreted with an integrative understanding of both local and far field effects.

## **Conclusion**

Here we present a comprehensive observation-based assessment describing the realised niche of diazotrophs in general and *Trichodesmium* in particular within the (sub)-tropical Atlantic. We interpret the prevailing Fe and P biogeochemistry of the region in terms of the well established resource ratio framework [Dutkiewicz *et al.*, 2012; Ward *et al.*, 2013]. In doing so we present further evidence supporting distinct diazotrophic provinces [Ward *et al.*, 2013] along observed antithetical Fe and P gradients. Such gradients appear to manifest at basin scales between the eastern and western SASG and inter-basin scales between the SASG and NASG. Highlighting a distinct lack of correlation between any one proposed environmental driving parameter (SST, pCO<sub>2</sub>, DIP or DFe) and diazotrophic activity and abundances, we emphasise how simple conceptual arguments and idealised numerical models assuming dual-control by Fe and P supply are entirely consistent with available observations. In particular, we suggest that observed L-shaped relationships between DFe and DIP in the Atlantic are both a consequence of and diagnostic of diazotroph-Fe-P feedbacks. By implication, the lack of such a relationship, if sampled over a sufficient range of ratios for total Fe and P supply, would have provided evidence for the absence of nutrient control and hence presumably dominance of other drivers of diazotrophy and reciprocally a reduced influence of diazotrophy on observed Fe and P distributions. Hence, while SST and pCO<sub>2</sub> may have an observed physiological effect on diazotroph and specifically *Trichodesmium* growth rates [Breitbarth *et al.*, 2007; Hutchins *et al.*, 2007; 2013; Fu *et al.*, 2014], in the extant (sub)-tropical Atlantic these effects are apparently overridden by nutrient (P, Fe) availability. These findings support the suggestion [Dutkiewicz *et al.*, 2014] that the resource ratio framework likely provides a strong basis for interpretation of past [Straub *et al.*, 2013] or predicted future changes [Luo *et al.*, 2013; Dutkiewicz *et al.*, 2014; Weber and Deutsch, 2014] in diazotrophy.

## **Acknowledgments:**

The data presented in this paper are available from either the British Oceanographic Data Centre (<http://www.bodc.ac.uk/>) or directly from J.T. Snow ([j.snow@noc.soton.ac.uk](mailto:j.snow@noc.soton.ac.uk)). The

work was supported by the UK Natural Environment Research Council (NERC) through a grant to the University of Southampton (NE/G015732/1) and National Capability funding to the Plymouth Marine Laboratory and the National Oceanography Centre, Southampton. The study is a UK contribution to the international SOLAS, GEOTRACES and IMBER projects. This is contribution number 260 of the AMT programme. We would like to thank D. Baker, S. Reynolds, V. Kitidis, D. Honey, E. Tynan, S. Ussher, M. Patey, M. Rijkenberg, S. Torres Valdes, U. Schuster, F. Malien, H. Luger, P. Fritsche, A. Kortzinger, P. Croot, C. Dumousseaud and B. Ward for their contributions towards data collection and discussion and two anonymous referees for their comments.

### References -

- Barcelos e Ramos, J., H. Biswas, K. G. Schulz, J. LaRoche, and U. Riebesell (2007), Effect of rising atmospheric carbon dioxide on the marine nitrogen fixer *Trichodesmium*, *Global Biogeochem. Cycles*, 21(2), n/a–n/a, doi:10.1029/2006GB002898.
- Berman-Frank, I., A. Quigg, Z. V. Finkel, A. J. Irwin, and L. Haramaty (2007), Nitrogen-fixation strategies and Fe requirements in cyanobacteria, *Limnol. Oceanogr.*, 52(5), 2260–2269, doi:10.4319/lo.2007.52.5.2260.
- Berman-Frank, I., P. Lundgren, Y. B. Chen, H. Küpper, Z. Kolber, B. Bergman, and P. Falkowski (2001), Segregation of nitrogen fixation and oxygenic photosynthesis in the marine cyanobacterium *Trichodesmium*, *Science*, 294(5546), 1534–1537, doi:10.1126/science.1064082.
- Bowie, A. R., D. J. Whitworth, E. P. Achterberg, R. Mantoura, and P. J. Worsfold (2002), Biogeochemistry of Fe and other trace elements (Al, Co, Ni) in the upper Atlantic Ocean, *Deep Sea Research Part I: Oceanographic Research Papers*, 49(4), 605–636, doi:10.1016/s0967-0637(01)00061-9.
- Boyd, P. W., Hunter, K. A., Jackson, G. A., E. Ibanami, E. Ibanami, S. G. Sander, and S. G. Sander (2010), Remineralization of upper ocean particles: Implications for iron biogeochemistry, *Limnol. Oceanogr.*, 55(3), 1271–1288, doi:10.4319/lo.2010.55.3.1271.
- Böttjer, D., D. M. Karl, R. M. Letelier, D. A. Viviani, and M. J. Church (2014), Experimental assessment of diazotroph responses to elevated seawater pCO<sub>2</sub> in the North Pacific Subtropical Gyre, *Global Biogeochem. Cycles*, 28(6), 601–616, doi:10.1002/2013GB004690.
- Breitbarth, E., A. Oschlies, and J. LaRoche (2007), Physiological constraints on the global distribution of *Trichodesmium* - effect of temperature on diazotrophy, *Biogeosciences*, 4(1), 53–61, doi:10.5194/bg-4-53-2007.
- Brewer, P. G., and J. P. Riley (1965), The automatic determination of nitrate in sea water, *Deep Sea Research and Oceanographic Abstracts*, 12(6), 765–772, doi:10.1016/0011-7471(65)90797-7.
- Broecker, W. S., and G. M. Henderson (1998), The sequence of events surrounding

- Termination II and their implications for the cause of glacial- interglacial CO<sub>2</sub> changes, *Paleoceanography*, 13(4), 352–364, doi:10.1029/98PA00920.
- Canfield, D. E. (2006), Models of oxic respiration, denitrification and sulfate reduction in zones of coastal upwelling, *Geochimica et Cosmochimica Acta*, 70(23), 5753–5765, doi:10.1016/j.gca.2006.07.023.
- Capone, D. G., J. A. Burns, J. P. Montoya, A. Subramaniam, C. Mahaffey, T. Gunderson, A. F. Michaels, and E. J. Carpenter (2005), Nitrogen fixation by *Trichodesmium* spp.: An important source of new nitrogen to the tropical and subtropical North Atlantic Ocean, *Global Biogeochem. Cycles*, 19(2), n/a–n/a, doi:10.1029/2004GB002331.
- Carpenter, E. J., A. Subramaniam, and D. G. Capone (2004), Biomass and primary productivity of the cyanobacterium *Trichodesmium* spp. in the tropical N Atlantic ocean, 51(2), 173–203, doi:10.1016/j.dsr.2003.10.006.
- Carvalho, M., S. M. F. Ganesella, and F. M. P. Saldanha-Corrêa (2008), *Trichodesmium erythraeum* Bloom on the Continental Shelf off Santos, Southeast Brazil, *Brazilian Journal of Oceanography*, 56(4), 307–311, doi:10.1590/S1679-87592008000400006.
- Codispoti, L. A. (2007), An oceanic fixed nitrogen sink exceeding 400 Tg N a<sup>-1</sup> vs the concept of homeostasis in the fixed-nitrogen inventory, *Biogeosciences*, 4(2), 233–253.
- Conway, T. M., Conway, T. M., S. G. John, and S. G. John (2014), Quantification of dissolved iron sources to the North Atlantic Ocean, *Nature*, 511(7508), 212–215, doi:10.1038/nature13482.
- Croot, P. L., P. Streu, and A. R. Baker (2004), Short residence time for iron in surface seawater impacted by atmospheric dry deposition from Saharan dust events, *Geophys. Res. Lett.*, 31(23), n/a–n/a, doi:10.1029/2004GL020153.
- Cullen, J. J. (1991), Hypotheses to explain high-nutrient conditions in the open sea, *Limnol. Oceanogr.*, 36(8), 1578–1599, doi:10.4319/lo.1991.36.8.1578.
- Dabundo, R., M. F. Lehmann, L. Treibergs, C. R. Tobias, M. A. Altabet, P. H. Moisander, and J. Granger (2014), The Contamination of Commercial 15N<sub>2</sub> Gas Stocks with 15N-Labeled Nitrate and Ammonium and Consequences for Nitrogen Fixation Measurements, *PLoS ONE*, 9(10), e110335, doi:10.1371/journal.pone.0110335.
- Deutsch, C., J. L. Sarmiento, D. M. Sigman, N. Gruber, and J. P. Dunne (2007), Spatial coupling of nitrogen inputs and losses in the ocean, *Nature*, 445(7124), 163–167, doi:10.1038/nature05392.
- Dickson, A. G., C. L. Sabine, and J. R. Christian (2007), *Guide to best practices for ocean CO<sub>2</sub> measurements*, PICES Special Publisher.
- Duce, R. A. et al. (2008), Impacts of atmospheric anthropogenic nitrogen on the open ocean, *Science*, 320(5878), 893–897, doi:10.1126/science.1150369.
- Dutkiewicz, S., B. A. Ward, F. Monteiro, and M. J. Follows (2012), Interconnection of nitrogen fixers and iron in the Pacific Ocean: Theory and numerical simulations, *Global Biogeochem. Cycles*, 26(1), n/a–n/a, doi:10.1029/2011GB004039.

- Dutkiewicz, S., B. A. Ward, J. R. Scott, and M. J. Follows (2014), Understanding predicted shifts in diazotroph biogeography using resource competition theory, *Biogeosciences Discuss.*, 11(5), 7113–7149, doi:10.5194/bgd-11-7113-2014.
- Dutkiewicz, S., M. J. Follows, and J. G. Bragg (2009), Modeling the coupling of ocean ecology and biogeochemistry, *Global Biogeochem. Cycles*, 23(4), n/a–n/a, doi:10.1029/2008GB003405.
- Dyhrman, S. T., P. D. Chappell, S. T. Haley, J. W. Moffett, E. D. Orchard, J. B. Waterbury, and E. A. Webb (2006), Phosphonate utilization by the globally important marine diazotroph *Trichodesmium*, *Nature*, 439(7072), 68–71, doi:10.1038/nature04203.
- Falkowski, P. G. (1997), Evolution of the nitrogen cycle and its influence on the biological sequestration of CO<sub>2</sub> in the ocean, *Nature*, 387(6630), 272–275, doi:10.1038/387272a0.
- Fernandez, A., B. Mouriño-Carballido, A. Bode, M. Varela, and E. Maranon (2010), Latitudinal distribution of *Trichodesmium* spp. and N<sub>2</sub> fixation in the Atlantic Ocean, *Biogeosciences*, 7(10), 3167–3176, doi:10.5194/bg-7-3167-2010.
- Foster, R. A., A. Subramaniam, C. Mahaffey, E. J. Carpenter, D. G. Capone, and J. P. Zehr (2007), Influence of the Amazon River plume on distributions of free-living and symbiotic cyanobacteria in the western tropical north Atlantic Ocean, *Limnol. Oceanogr.*, 52(2), 517–532, doi:10.4319/lo.2007.52.2.0517.
- Fu, F. X., E. Yu, N. S. Garcia, J. Gale, Y. Luo, E. A. Webb, and D. A. Hutchins (2014), Differing responses of marine N<sub>2</sub> fixers to warming and consequences for future diazotroph community structure, *Aquat. Microb. Ecol.*, 72(1), 33–46, doi:10.3354/ame01683.
- Garcia, N. S., F. Fu, P. N. Sedwick, and D. A. Hutchins (2015), Iron deficiency increases growth and nitrogen-fixation rates of phosphorus-deficient marine cyanobacteria, *The ISME Journal*, 9(1), 238–245, doi:10.1038/ismej.2014.104.
- Garcia, N. S., F. X. Fu, and D. A. Hutchins (2013), Colimitation of the unicellular photosynthetic diazotroph *Crocospaera watsonii* by phosphorus, light, and carbon dioxide, *Limnol Oceanogr.*
- Goebel, N. L., K. A. Turk, K. M. Achilles, R. Paerl, I. Hewson, A. E. Morrison, J. P. Montoya, C. A. Edwards, and J. P. Zehr (2010), Abundance and distribution of major groups of diazotrophic cyanobacteria and their potential contribution to N<sub>2</sub> fixation in the tropical Atlantic Ocean, *Environ Microbiol*, 12(12), 3272–3289, doi:10.1111/j.1462-2920.2010.02303.x.
- Gradoville, M. R., A. E. White, D. Böttjer, and M. J. Church (2014), Diversity trumps acidification: Lack of evidence for carbon dioxide enhancement of *Trichodesmium* community nitrogen or carbon fixation at Station ALOHA, *Limnology and Oceanography*, 59(3), 645–659.
- Grasshoff, K., K. Kremling, and M. Ehrhardt (1976), *Methods of Seawater Analysis*, John Wiley and Sons.
- Graziano, L. M., R. J. Geider, W. Li, and M. Olaizola (1996), Nitrogen limitation of North

Atlantic phytoplankton: Analysis of physiological condition in nutrient enrichment experiments, *Aquat. Microb. Ecol.*, 11(1), 53–64, doi:10.3354/ame011053.

Großkopf, T., W. Mohr, T. Baustian, H. Schunck, D. Gill, M. M. M. Kuypers, G. Lavik, R. A. Schmitz, D. W. R. Wallace, and J. LaRoche (2012), Doubling of marine dinitrogen-fixation rates based on direct measurements, *Nature*, 488(7411), 361–364, doi:10.1038/nature11338.

Gruber, N. (2008), *The Marine Nitrogen Cycle*, Elsevier.

Hardman-Mountford, N. J. et al. (2008), An operational monitoring system to provide indicators of CO<sub>2</sub>-related variables in the ocean, *ICES Journal of Marine Science*, 65(8), 1498–1503, doi:10.1093/icesjms/fsn110.

Huertas, I. E., M. Rouco, V. López-Rodas, and E. Costas (2011), Warming will affect phytoplankton differently: evidence through a mechanistic approach, *Proc. Biol. Sci.*, 278(1724), 3534–3543, doi:10.1098/rspb.2011.0160.

Hutchins, D. A., F. X. Fu, Y. Zhang, M. E. Warner, Y. Feng, K. Portune, P. W. Bernhardt, and M. R. Mulholland (2007), CO<sub>2</sub> control of Trichodesmium N<sub>2</sub> fixation, photosynthesis, growth rates, and elemental ratios: Implications for past, present, and future ocean biogeochemistry, *Limnol. Oceanogr.*, 52(4), 1293–1304, doi:10.4319/lo.2007.52.4.1293.

Hutchins, D. A., F.-X. Fu, E. A. Webb, N. Walworth, and A. Tagliabue (2013), Taxon-specific response of marine nitrogen fixers to elevated carbon dioxide concentrations, *Nature Geosci.*, 6(9), 790–795, doi:10.1038/ngeo1858.

Jickells, T. (2006), The role of air-sea exchange in the marine nitrogen cycle, *Biogeosciences*, 3(3), 271–280, doi:10.5194/bg-3-271-2006.

Jickells, T. D. et al. (2005), Global iron connections between desert dust, ocean biogeochemistry, and climate, *Science*, 308(5718), 67–71, doi:10.1126/science.1105959.

Kitidis, V. et al. (2012), Seasonal dynamics of the carbonate system in the Western English Channel, *Continental Shelf Research*, 42, 30–40, doi:10.1016/j.csr.2012.04.012.

Klunder, M. B., P. Laan, R. Middag, H. J. W. De Baar, and J. C. van Ooijen (2011), Dissolved iron in the Southern Ocean (Atlantic sector), *Deep Sea Research Part II: Topical Studies in Oceanography*, 58(25-26), 2678–2694, doi:10.1016/j.dsr2.2010.10.042.

Körtzinger, A. (1999), *Determination of carbon dioxide partial pressure (p(CO<sub>2</sub>))*, Wiley-VCH Verlag GmbH, Weinheim, Germany.

Kranz, S. A., D. Sültemeyer, K.-U. Richter, and B. Rost (2009), Carbon acquisition by Trichodesmium: the effect of pCO<sub>2</sub> and diurnal changes, *Limnol. Oceanogr.*, 54(2), 548–559, doi:10.4319/lo.2009.54.2.0548.

Kranz, S. A., D. Wolf-Gladrow, G. Nehrke, G. Langer, and B. Rost (2010), Calcium carbonate precipitation induced by the growth of the marine cyanobacteria Trichodesmium, *Limnol. Oceanogr.*, 55(6), 2563–2569, doi:10.4319/lo.2010.55.6.2563.



- Landolfi, A., H. Dietze, W. Koeve, and A. Oschlies (2013), Overlooked runaway feedback in the marine nitrogen cycle: the vicious cycle, *Biogeosciences*, 10(3), 1351–1363, doi:10.5194/bg-10-1351-2013.
- LaRoche, J., and E. Breitbarth (2005), Importance of the diazotrophs as a source of new nitrogen in the ocean, *Journal of Sea Research*, 53(1-2), 67–91, doi:10.1016/j.seares.2004.05.005.
- Lomas, M. W., A. L. Burke, D. A. Lomas, D. W. Bell, C. Shen, S. T. Dyrhman, and J. W. Ammerman (2010), Sargasso Sea phosphorus biogeochemistry: an important role for dissolved organic phosphorus (DOP), *Biogeosciences*, 7(2), 695–710, doi:10.5194/bg-7-695-2010.
- Luo, Y. W. et al. (2012), Database of diazotrophs in global ocean: abundance, biomass and nitrogen fixation rates, *Earth System Science Data*, 4(1), 47–73, doi:10.5194/essd-4-47-2012.
- Luo, Y. W., I. D. Lima, D. M. Karl, and S. C. Doney (2013), Data-based assessment of environmental controls on global marine nitrogen fixation, *Biogeosciences Discuss.*, 10(4), 7367–7412, doi:10.5194/bgd-10-7367-2013.
- Mahaffey, C., A. F. Michaels, and D. G. Capone (2005), The conundrum of marine N<sub>2</sub> fixation, *American Journal of Science*, 305(6-8), 546–595, doi:10.2475/ajs.305.6-8.546.
- Mahaffey, C., S. Reynolds, C. E. Davis, and M. C. Lohan (2014), Alkaline phosphatase activity in the subtropical ocean: insights from nutrient, dust and trace metal addition experiments, *Front. Mar. Sci.*, 1, doi:10.3389/fmars.2014.00073.
- Martino, M., D. Hamilton, A. R. Baker, T. D. Jickells, T. Bromley, Y. Nojiri, B. Quack, and P. W. Boyd (2014), Western Pacific atmospheric nutrient deposition fluxes, their impact on surface ocean productivity, *Global Biogeochem. Cycles*, 28(7), 712–728, doi:10.1002/2013GB004794.
- Mather, R. L., S. E. Reynolds, G. A. Wolff, S. Torres-Valdes, E. M. S. Woodward, A. Landolfi, X. Pan, R. Sanders, and E. P. Achterberg (2008), Phosphorus cycling in the North and South Atlantic Ocean subtropical gyres, *Nature Geosci.*, 1(7), 439–443, doi:10.1038/ngeo232.
- McLaughlin, K., J. A. Sohm, G. A. Cutter, M. W. Lomas, and A. Paytan (2013), Phosphorus cycling in the Sargasso Sea: Investigation using the oxygen isotopic composition of phosphate, enzyme-labeled fluorescence, and turnover times, *Global Biogeochem. Cycles*, 27(2), 375–387, doi:10.1002/gbc.20037.
- Mills, M. M., C. Ridame, M. Davey, J. La Roche, and R. J. Geider (2004), Iron and phosphorus co-limit nitrogen fixation in the eastern tropical North Atlantic, *Nature*, 429(6989), 292–294, doi:10.1038/nature02550.
- Milne, A., W. Landing, M. Bizimis, and P. Morton (2010), Determination of Mn, Fe, Co, Ni, Cu, Zn, Cd and Pb in seawater using high resolution magnetic sector inductively coupled mass spectrometry (HR-ICP-MS), *Analytica Chimica Acta*, 665(2), 200–207, doi:10.1016/j.aca.2010.03.027.



- Mitchell, T. P., and J. M. Wallace (1992), The Annual Cycle in Equatorial Convection and Sea Surface Temperature, *Journal of Climate*, 5(10), 1140–1156, doi:10.1175/1520-0442(1992)005<1140:taciec>2.0.co;2.
- Mohr, W., T. Großkopf, D. W. R. Wallace, and J. LaRoche (2010), Methodological underestimation of oceanic nitrogen fixation rates., edited by Z. Finkel, *PLoS ONE*, 5(9), doi:10.1371/journal.pone.0012583.
- Moisan, P. H., R. A. Beinart, I. Hewson, A. E. White, K. S. Johnson, C. A. Carlson, J. P. Montoya, and J. P. Zehr (2010), Unicellular cyanobacterial distributions broaden the oceanic N<sub>2</sub> fixation domain, *Science*, 327(5972), 1512–1514, doi:10.1126/science.1185468.
- Monteiro, F. M., M. J. Follows, and S. Dutkiewicz (2010), Distribution of diverse nitrogen fixers in the global ocean, *Global Biogeochem. Cycles*, 24(3), n/a–n/a, doi:10.1029/2009GB003731.
- Monteiro, F. M., S. Dutkiewicz, and M. J. Follows (2011), Biogeographical controls on the marine nitrogen fixers, *Global Biogeochem. Cycles*, 25(2), n/a–n/a, doi:10.1029/2010GB003902.
- Montoya, J. P., C. M. Holl, J. P. Zehr, A. Hansen, T. A. Villareal, and D. G. Capone (2004), High rates of N<sub>2</sub> fixation by unicellular diazotrophs in the oligotrophic Pacific Ocean, *Nature*, 430(7003), 1027–1032, doi:10.1038/nature02824.
- Montoya, J. P., M. Voss, P. Kahler, and D. G. Capone (1996), A Simple, High-Precision, High-Sensitivity Tracer Assay for N<sub>2</sub> Fixation, *Applied and Environmental Microbiology*, 62(3), 986–993.
- Moore, C. M. et al. (2013), Processes and patterns of oceanic nutrient limitation, *Nature Geosci*, 6(March), 701–710.
- Moore, C. M. et al. (2009), Large-scale distribution of Atlantic nitrogen fixation controlled by iron availability, *Nature Geosci*, 2(12), 867–871, doi:10.1038/ngeo667.
- Moore, C. M., M. M. Mills, A. Milne, R. LANGLOIS, E. P. Achterberg, K. LOCHTE, R. J. Geider, and J. La Roche (2006), Iron limits primary productivity during spring bloom development in the central North Atlantic, *Glob Change Biol*, 12(4), 626–634, doi:10.1111/j.1365-2486.2006.01122.x.
- Moore, C. M., M. M. Mills, R. LANGLOIS, A. Milne, E. P. Achterberg, J. La Roche, and R. J. Geider (2008), Relative influence of nitrogen and phosphorous availability on phytoplankton physiology and productivity in the oligotrophic sub-tropical North Atlantic Ocean, *Limnol. Oceanogr.*, 53(1), 291–305, doi:10.4319/lo.2008.53.1.0291.
- Moore, J. K., and O. Braucher (2008), Sedimentary and mineral dust sources of dissolved iron to the world ocean, *Biogeosciences*, 5(3), 631–656.
- Moore, R. M., M. Kienast, M. Fraser, J. J. Cullen, C. Deutsch, S. Dutkiewicz, M. J. Follows, and C. J. Somes (2014), Extensive hydrogen supersaturations in the western South Atlantic Ocean suggest substantial underestimation of nitrogen fixation, *J. Geophys. Res.*

*Oceans*, 119(7), 4340–4350, doi:10.1002/2014JC010017.

Orchard, E. D., C. R. Benitez-Nelson, P. J. Pellechia, M. W. Lomas, and S. T. Dyrman (2010), Polyphosphate in *Trichodesmium* from the low-phosphorus Sargasso Sea, *Limnol. Oceanogr.*, 55(5), 2161–2169, doi:10.4319/lo.2010.55.5.2161.

Orchard, E. D., E. A. Webb, and S. T. Dyrman (2009), Molecular analysis of the phosphorus starvation response in *Trichodesmium* spp, *Environ Microbiol*, 11(9), 2400–2411, doi:10.1111/j.1462-2920.2009.01968.x.

Palter, J. B., J. L. Sarmiento, and A. Gnanadesikan (2010), Fueling export production: nutrient return pathways from the deep ocean and their dependence on the Meridional Overturning Circulation, *Biogeosciences*, 7(11), 3549–3568, doi:10.5194/bg-7-3549-2010.

Pandey, K. D., S. P. Shukla, P. N. Shukla, D. D. Giri, J. S. Singh, P. Singh, and A. K. Kashyap (2004), Cyanobacteria in Antarctica: ecology, physiology and cold adaptation, *Cell. Mol. Biol. (Noisy-le-grand)*, 50(5), 575–584.

Patey, M. D., M. J. A. Rijkenberg, P. J. Statham, M. C. Stinchcombe, E. P. Achterberg, and M. Mowlem (2008), Determination of nitrate and phosphate in seawater at nanomolar concentrations, *TrAC Trends in Analytical Chemistry*, 27(2), 169–182, doi:10.1016/j.trac.2007.12.006.

Philander, S. G. H., D. Gu, G. Lambert, T. Li, D. Halpern, N.-C. Lau, and R. C. Pacanowski (1996), Why the ITCZ Is Mostly North of the Equator, *Journal of Climate*, 9(12), 2958–2972, doi:10.1175/1520-0442(1996)009<2958:wtiimn>2.0.co;2.

Raven, J. A. (1988), The iron and molybdenum use efficiencies of plant growth with different energy, carbon and nitrogen sources, *New Phytologist*, 109(3), 279–287, doi:10.1111/j.1469-8137.1988.tb04196.x.

Reynolds, S., C. Mahaffey, V. Roussenov, and R. G. Williams (2014), Evidence for production and lateral transport of dissolved organic phosphorus in the eastern subtropical North Atlantic, *Global Biogeochem. Cycles*, 28(8), 805–824, doi:10.1002/2013GB004801.

Richier, S., A. I. Macey, N. J. Pratt, D. J. Honey, C. M. Moore, and T. S. Bibby (2012), Abundances of iron-binding photosynthetic and nitrogen-fixing proteins of *Trichodesmium* both in culture and in situ from the North Atlantic., edited by L. J. Stal, *PLoS ONE*, 7(5), e35571, doi:10.1371/journal.pone.0035571.

Rijkenberg, M. J. A., S. Steigenberger, C. F. Powell, H. van Haren, M. D. Patey, A. R. Baker, and E. P. Achterberg (2012), Fluxes and distribution of dissolved iron in the eastern (sub-) tropical North Atlantic Ocean, *Global Biogeochem. Cycles*, 26(3), n/a–n/a, doi:10.1029/2011GB004264.

Roy, N. K., R. K. Ghosh, and J. Das (1982), Monomeric alkaline phosphatase of *Vibrio cholerae*, *Journal of Bacteriology*, 150(3), 1033–1039.

Rödenbeck, C., R. F. Keeling, D. C. E. Bakker, N. Metzl, C. Sabine, and M. Heimann (2013), Global surface-ocean pCO<sub>2</sub> and sea–air CO<sub>2</sub> flux variability from an observation-driven

- ocean mixed-layer scheme, *Ocean Sci.*, 9(2), 193–216, doi:10.5194/os-9-193-2013.
- Ryther, J. H., and W. M. Dunstan (1971), Nitrogen, phosphorus, and eutrophication in the coastal marine environment, *Science*, 171(3975), 1008–1013, doi:10.1126/science.171.3975.1008.
- Saito, M. A., A. E. Noble, A. Tagliabue, T. J. Goepfert, C. H. Lamborg, and W. J. Jenkins (2013), Slow-spreading submarine ridges in the South Atlantic as a significant oceanic iron source, *Nature Geosci*, 6(9), 775–779, doi:10.1038/ngeo1893.
- Saito, M. A., S. Dutkiewicz, V. V. Bulygin, D. M. Moran, M. J. Follows, and J. B. Waterbury (2011), Iron conservation by reduction of metalloenzyme inventories in the marine diazotroph *Crocospaera watsonii*, *Proc. Natl. Acad. Sci. U.S.A.*, 108(6), 2184–2189, doi:10.1073/pnas.1006943108.
- Sandh, G., R. El-Shehawy, B. Díez, and B. Bergman (2009), Temporal separation of cell division and diazotrophy in the marine diazotrophic cyanobacterium *Trichodesmium erythraeum* IMS101, *FEMS Microbiology Letters*, 295(2), 281–288, doi:10.1111/j.1574-6968.2009.01608.x.
- Sañudo-Wilhelmy, S. A., A. B. Kustka, C. J. Gobler, D. A. Hutchins, M. Yang, K. Lwiza, J. Burns, D. G. Capone, J. A. Raven, and E. J. Carpenter (2001), Phosphorus limitation of nitrogen fixation by *Trichodesmium* in the central Atlantic Ocean, *Nature*, 411(6833), 66–69, doi:10.1038/35075041.
- Schlosser, C., J. K. Klar, B. D. Wake, J. T. Snow, D. J. Honey, E. M. S. Woodward, M. C. Lohan, E. P. Achterberg, and C. M. Moore (2014), Seasonal ITCZ migration dynamically controls the location of the (sub)tropical Atlantic biogeochemical divide, *Proc. Natl. Acad. Sci. U.S.A.*, 111(4), 1438–1442, doi:10.1073/pnas.1318670111.
- Shi, Y. Sun, and P. G. Falkowski (2007), Effects of iron limitation on the expression of metabolic genes in the marine cyanobacterium *Trichodesmium erythraeum* IMS101, *Environ Microbiol*, 9(12), 2945–2956, doi:10.1111/j.1462-2920.2007.01406.x.
- Sohm, J. A., A. Subramaniam, T. E. Gunderson, E. J. Carpenter, and D. G. Capone (2011a), Nitrogen fixation by *Trichodesmium* spp. and unicellular diazotrophs in the North Pacific Subtropical Gyre, *Journal of Geophysical Research: Biogeosciences (2005–2012)*, 116(G3), G03002, doi:10.1029/2010JG001513.
- Sohm, J. A., C. Mahaffey, and D. G. Capone (2008), Assessment of relative phosphorus limitation of *Trichodesmium* spp. in the North Pacific, North Atlantic, and the north coast of Australia, *Limnol. Oceanogr.*, 53(6), 2495–2502, doi:10.4319/lo.2008.53.6.2495.
- Sohm, J. A., E. A. Webb, and D. G. Capone (2011b), Emerging patterns of marine nitrogen fixation, *Nat Rev Micro*, 9(7), 499–508, doi:10.1038/nrmicro2594.
- Sohm, J. A., J. A. Hilton, A. E. Noble, J. P. Zehr, M. A. Saito, and E. A. Webb (2011c), Nitrogen fixation in the South Atlantic Gyre and the Benguela Upwelling System, *Geophys. Res. Lett.*, 38(16), n/a–n/a, doi:10.1029/2011GL048315.
- Staal, M., F. J. R. Meysman, and L. J. Stal (2003), Temperature excludes N<sub>2</sub>-fixing heterocystous cyanobacteria in the tropical oceans, *Nature*, 425(6957), 504–507,

doi:10.1038/nature01999.

- Stal, L. J. (2009), Is the distribution of nitrogen-fixing cyanobacteria in the oceans related to temperature? *Environ Microbiol*, *11*(7), 1632–1645, doi:10.1111/j.1758-2229.2009.00016.x.
- Straub, M., D. M. Sigman, H. Ren, A. Martínez-García, A. N. Meckler, M. P. Hain, and G. H. Haug (2013), Changes in North Atlantic nitrogen fixation controlled by ocean circulation, *Nature*, *501*(7466), 200–203, doi:10.1038/nature12397.
- Subramaniam, A. et al. (2008), Amazon River enhances diazotrophy and carbon sequestration in the tropical North Atlantic Ocean, *Proc. Natl. Acad. Sci. U.S.A.*, *105*(30), 10460–10465, doi:10.1073/pnas.0710279105.
- Thomas, M. K., C. T. Kremer, C. A. Klausmeier, and E. Litchman (2012), A global pattern of thermal adaptation in marine phytoplankton, *Science*, *338*(6110), 1085–1088, doi:10.1126/science.1224836.
- Tilman, D. (1980), Resources: A Graphical-Mechanistic Approach to Competition and Predation, *The American Naturalist*, *116*(3), 362, doi:10.1086/283633.
- Tilman, D., S. S. Kilham, and P. Kilham (1982), Phytoplankton Community Ecology: The Role of Limiting Nutrients, *Annual Review of Ecology and Systematics*, *13*(1), 349–372, doi:10.1146/annurev.es.13.110182.002025.
- Tyrrell, T. (1999), The relative influences of nitrogen and phosphorus on oceanic primary production, *Nature*, *400*(6744), 525–531, doi:10.1038/22941.
- Tyrrell, T., E. Marañón, A. J. Poulton, D. S. Harbour, and E. M. S. Woodward (2003), Large-scale latitudinal distribution of *Trichodesmium* spp. in the Atlantic Ocean, *Journal of Plankton Research*, *25*(4), 405–416, doi:10.1093/plankt/25.4.405.
- Van Mooy, B. A. S. et al. (2009), Phytoplankton in the ocean use non-phosphorus lipids in response to phosphorus scarcity, *Nature*, *458*(7234), 69–72, doi:10.1038/nature07659.
- Ward, B. A., S. Dutkiewicz, C. M. Moore, and M. J. Follows (2013), Iron, phosphorus, and nitrogen supply ratios define the biogeography of nitrogen fixation, *Limnol. Oceanogr.*, *58*(6), 2059–2075, doi:10.4319/lo.2013.58.6.2059.
- Weber, T., and C. Deutsch (2014), Local versus basin-scale limitation of marine nitrogen fixation, *Proc. Natl. Acad. Sci. U.S.A.*, *111*(24), 8741–8746, doi:10.1073/pnas.1317193111.
- Wilson, S. T., Z. S. Kolber, S. Tozzi, J. P. Zehr, and D. M. Karl (2012), NITROGEN FIXATION, HYDROGEN CYCLING, AND ELECTRON TRANSPORT KINETICS IN TRICHODESMIUM ERYTHRAEUM (CYANOBACTERIA) STRAIN IMS1011, *J Phycol*, *48*(3), 595–606, doi:10.1111/j.1529-8817.2012.01166.x.
- Wu, J. (2000), Phosphate Depletion in the Western North Atlantic Ocean, *Science*, *289*(5480), 759–762, doi:10.1126/science.289.5480.759.
- Wurl, O., L. Zimmer, and G. A. Cutter (2013), Arsenic and phosphorus biogeochemistry in

the ocean: Arsenic species as proxies for P-limitation, *Limnol Oceanogr*,  
doi:10.4319/lo.2013.58.2.0729.

Xie, S.-P., and K. Saito (2001), Formation and Variability of a Northerly ITCZ in a Hybrid Coupled AGCM: Continental Forcing and Oceanic–Atmospheric Feedback\*, *Journal of Climate*, 14(6), 1262–1276, doi:10.1175/1520-0442(2001)014<1262:favoan>2.0.co;2.

Zehr, J. P. (2011), Nitrogen fixation by marine cyanobacteria, *Trends Microbiol.*, 19(4), 162–173, doi:10.1016/j.tim.2010.12.004.

Accepted Article

**Table 1: Coefficients of determination**

Coefficient of determination ( $R^2$ ) for either community  $N_2$  fixation or *Trichodesmium* abundance compared with SST,  $pCO_2$ , DFe and DIP in paired samples. Sample size is shown in brackets, significant correlation as determined by Student's t-test ( $P < 0.01$ ) are highlighted in bold font.

Parameter	Community $N_2$ Fixation	Trichodesmium Abundance
SST	0.03 (n=107)	0.01 (n=79)
$pCO_2$	0.02 (n=95)	0.09 (n=70)
DFe	0.04 (n=69)	0.00 (n=62)
DIP	<b>0.06 (n=105)</b>	0.07 (n=74)

Accepted Article



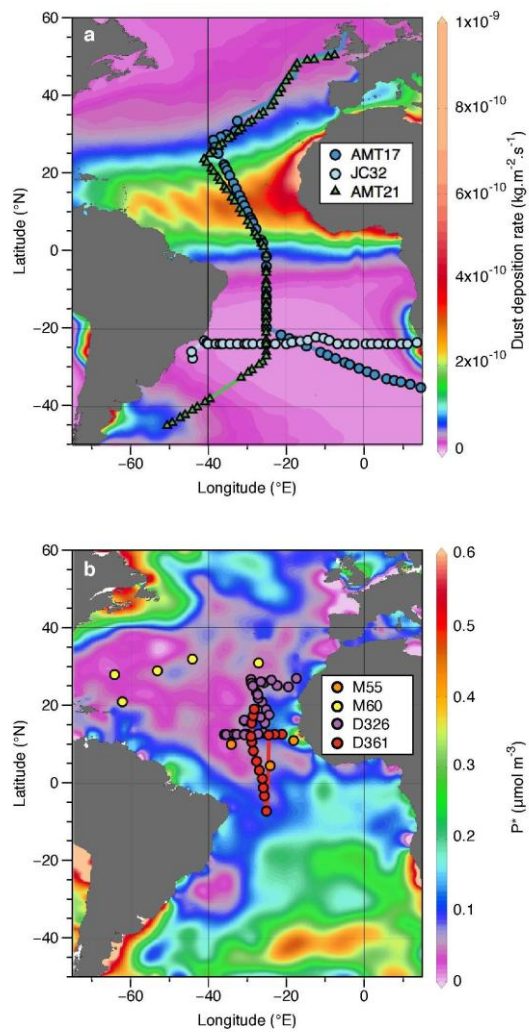


**Figure 1** - Cruise transects for the 7 cruises included in this study. Transects are overlaid on A) the modelled annual average dust deposition rate ( $\text{kg m}^{-2} \text{s}^{-1}$ ), re-plotted from [Mahowald *et al.*, 2005] or B)  $P^* = \text{DIP-DIN}/16$  from the WOCE Ocean Atlas. Cruises are separated across maps for clarity.

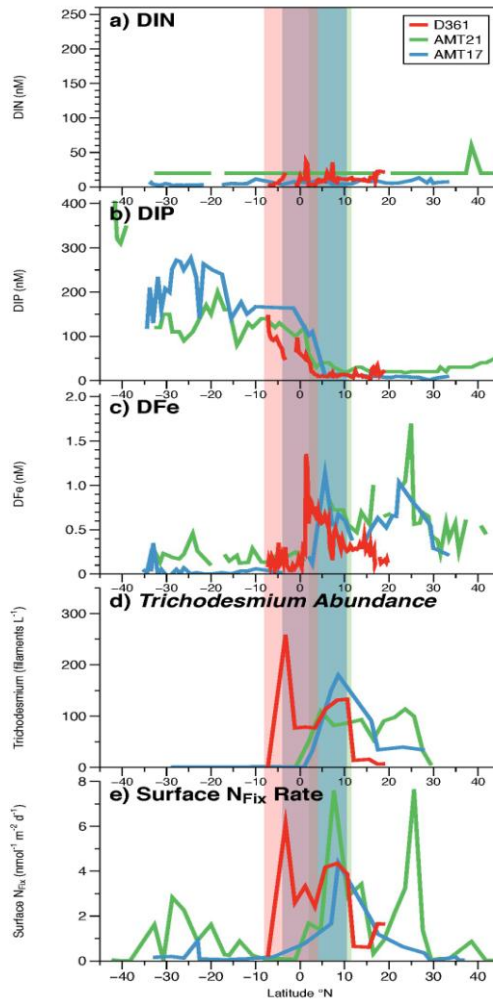


**Figure 2** - Previously unpublished data collected along an Atlantic Meridional Transect (AMT21, green) at  $\sim 25^{\circ}\text{W}$  during northern hemisphere spring and autumn compared with two previous cruises, AMT17 (blue) and D361 (red). A) Dissolved inorganic nitrogen, DIN (nM), B) Dissolved inorganic phosphorus, DIP (nM), C) Dissolved iron, DFe (nM), D) *Trichodesmium* abundance (Trichomes  $\text{L}^{-1}$ ) E) Whole community surface  $\text{N}_2$  fixation rates ( $\text{nmol m}^{-2} \text{d}^{-1}$ ). Shaded regions represent enhanced surface rainfall as defined by precipitation  $>2 \times 10^{-5} \text{ Kg m}^{-2} \text{ s}^{-1}$  as derived from NCEP reanalysis daily average surface flux data. The enhanced precipitation region indicated the approximate location of the ITCZ during AMT17 (15<sup>th</sup> October – 28<sup>th</sup> November 2005, blue), D361 (7<sup>th</sup> February - 19<sup>th</sup> March 2011, red) and AMT21 (29<sup>th</sup> September - 14<sup>th</sup> November 2011, green).

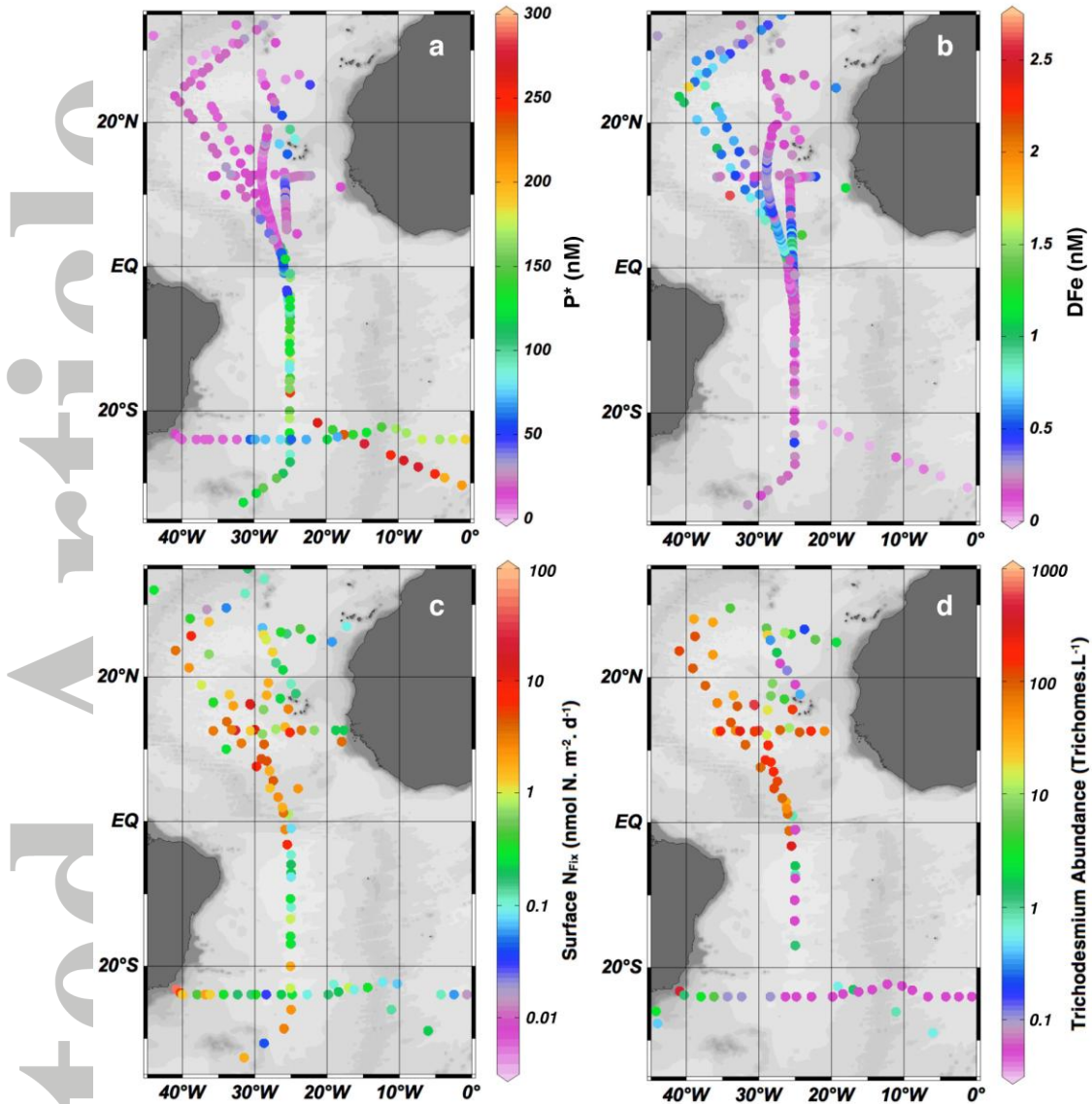


**Figure 3** - Data collected from cruises M55 (Oct-Nov 2002, R/V Meteor), M60 (Nov-Dec 2003, R/V Meteor), AMT17 (Oct-Nov 2005, RRS Discovery), D326 (Jan-Feb 2008, RRS James Cook), JC32 (Mar-May 2009, RRS James Cook), D361 (Feb-Mar 2011, RRS Discovery) and AMT21 (Oct-Nov 2011, RRS Discovery). A)  $P^*$  (nM) =  $\text{DIP-DIN}/r_{\text{N/P}}$ , B) Dissolved iron, DFe (nM), C) Whole community surface  $\text{N}_2$  fixation ( $\text{nmol m}^{-2} \text{d}^{-1}$ ), D) *Trichodesmium* abundance ( $\text{Trichomes L}^{-1}$ ).

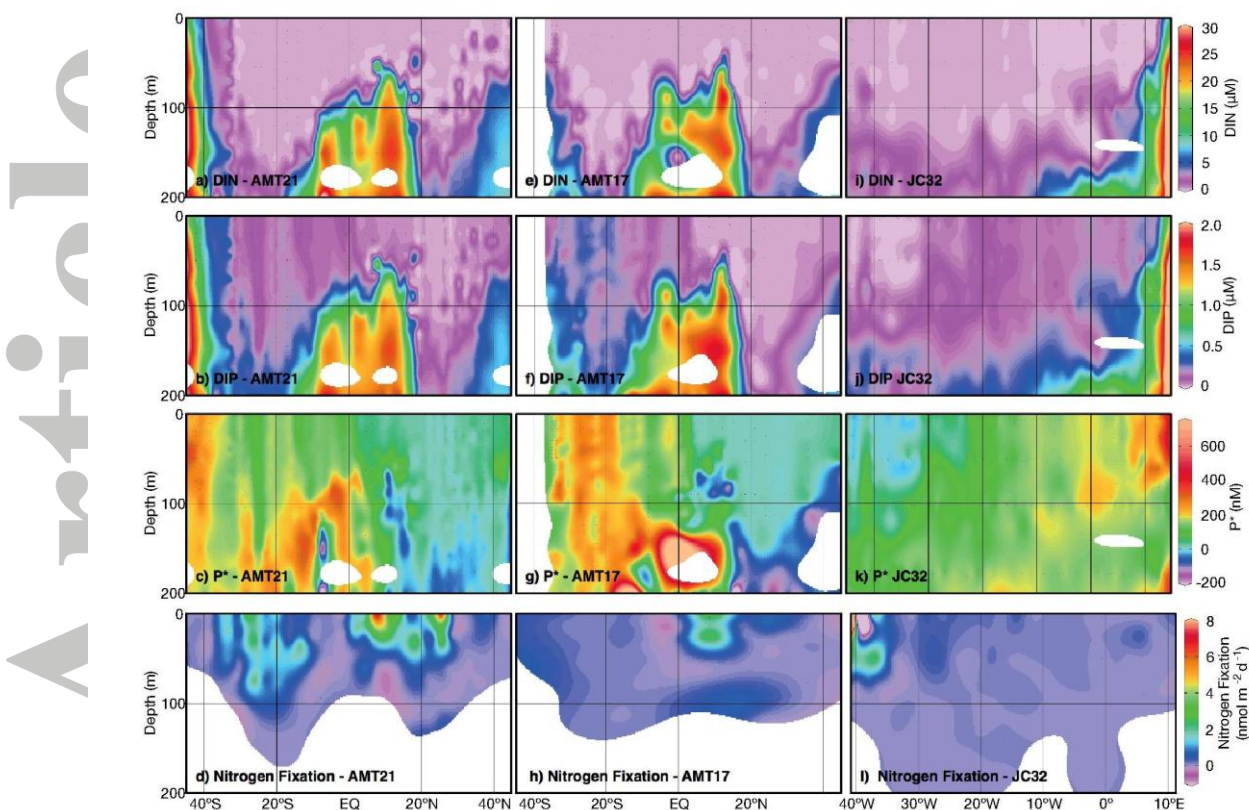


**Figure 4** - Contour plots presenting DIN (nM), DIP (nM), P\* (nM) and N<sub>2</sub> fixation rates (nmol m<sup>-2</sup> d<sup>-1</sup>) within the euphotic zone for AMT21 (A,B,C and D respectively), AMT17 (E, F, G and H respectively) and JC32 (I, J, K and L respectively), with data from AMT21 and JC32 being previously unpublished. Red lines indicate points of cruise intersection with JC32 crossing the AMT21 transect at ~25 °E, crossing AMT17 at ~17.25 °E. AMT17 and AMT21 both cross the JC32 transect at ~24-25 °N.

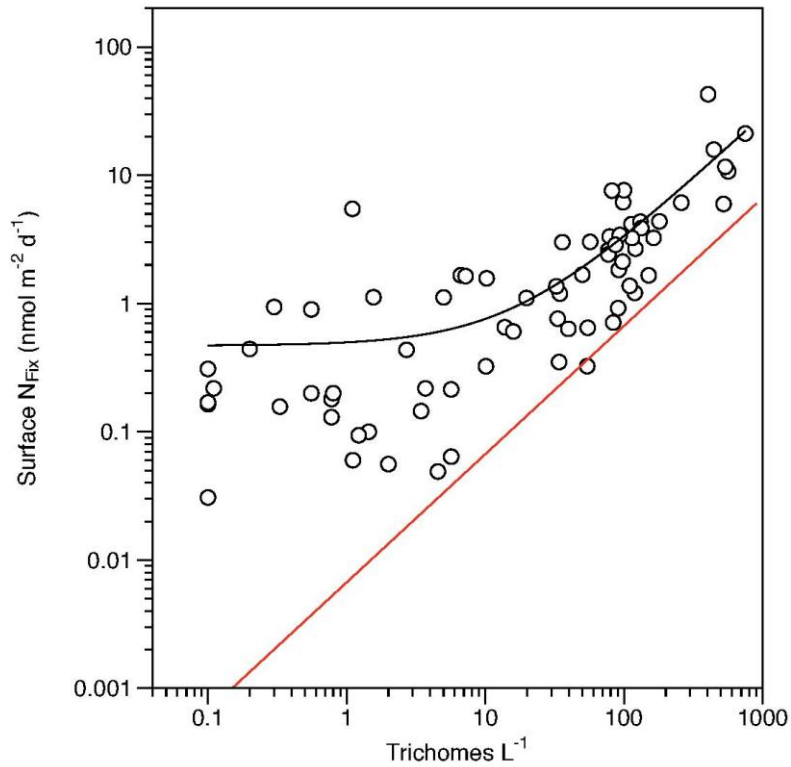


**Figure 5** - Correlation between *Trichodesmium* abundance (Trichomes L<sup>-1</sup>) and whole community N<sub>2</sub> fixation rates (nmol N m<sup>-2</sup> d<sup>-1</sup>) shown in black, R<sup>2</sup>=0.86. Measured mean N<sub>2</sub> fixation per trichome (nmol N Trichome<sup>-1</sup> d<sup>-1</sup>) shown in red.



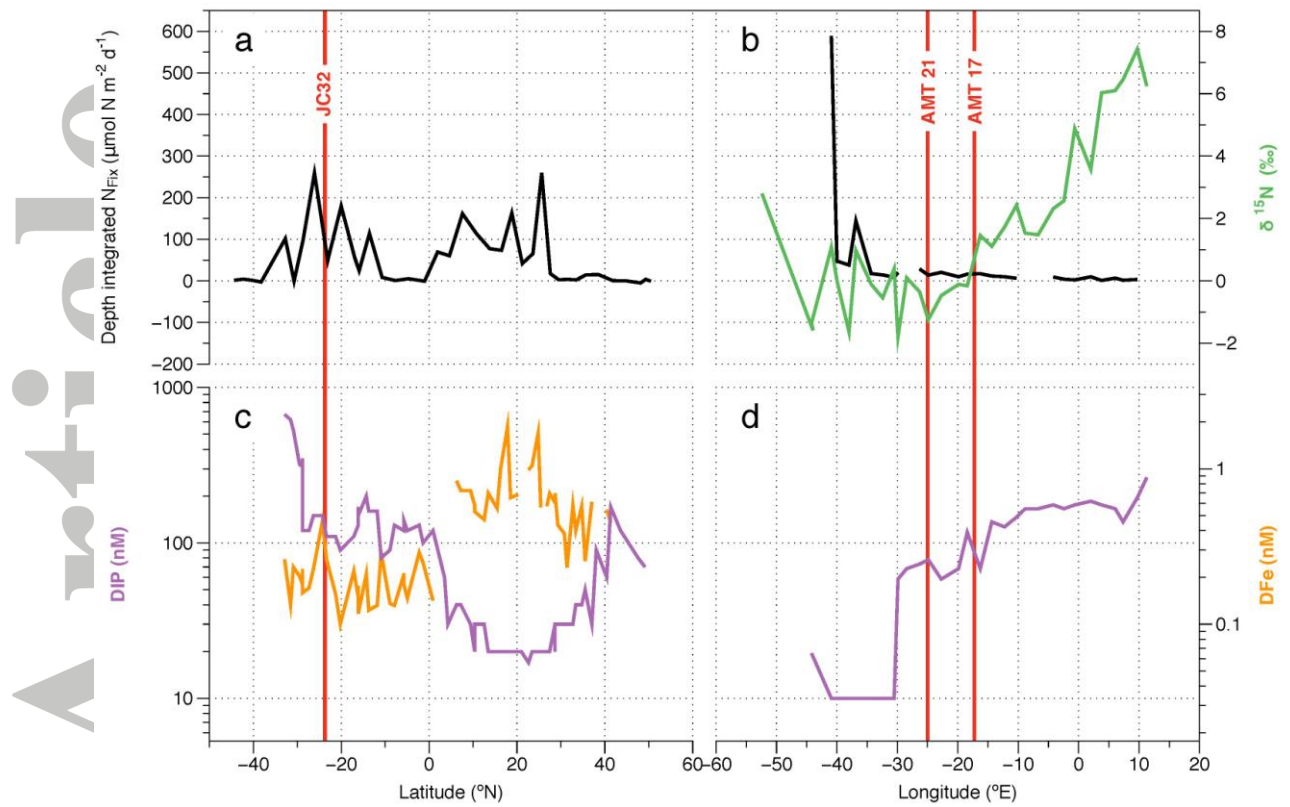


**Figure 6** - Depth integrated  $\text{N}_2$  fixation rates and  $\delta^{15}\text{PON}$  natural abundance data observed during AMT21 (A,  $\text{N}_2$  fixation only) and JC32 (B). DFe (orange) and DIP (purple) surface water concentrations observed during AMT21 (C) and JC32 (D, DIP only).

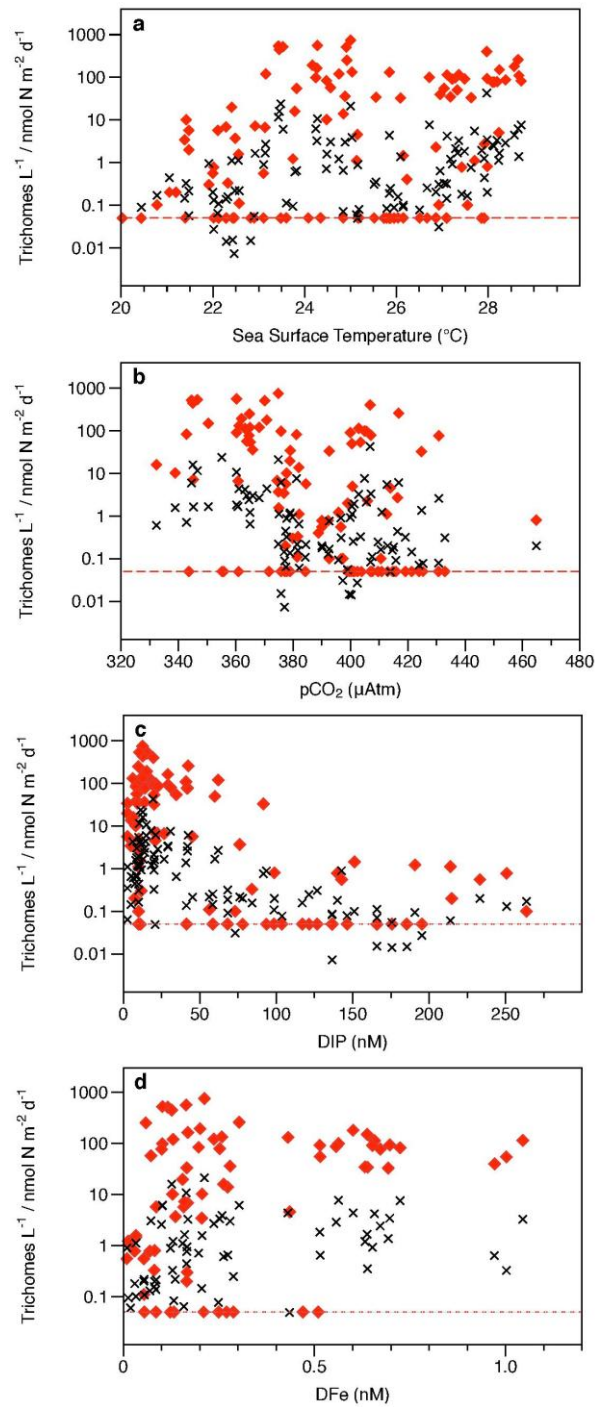


**Figure 7** - *Trichodesmium* abundance (Trichomes L<sup>-1</sup>) (black crosses) and whole community N<sub>2</sub> fixation rates (nmol m<sup>-2</sup> d<sup>-1</sup>) (red diamonds) as a function of observed A) SST (°C), B) pCO<sub>2</sub> (µatm), C) DIP (nM) or D) DFe (nM).

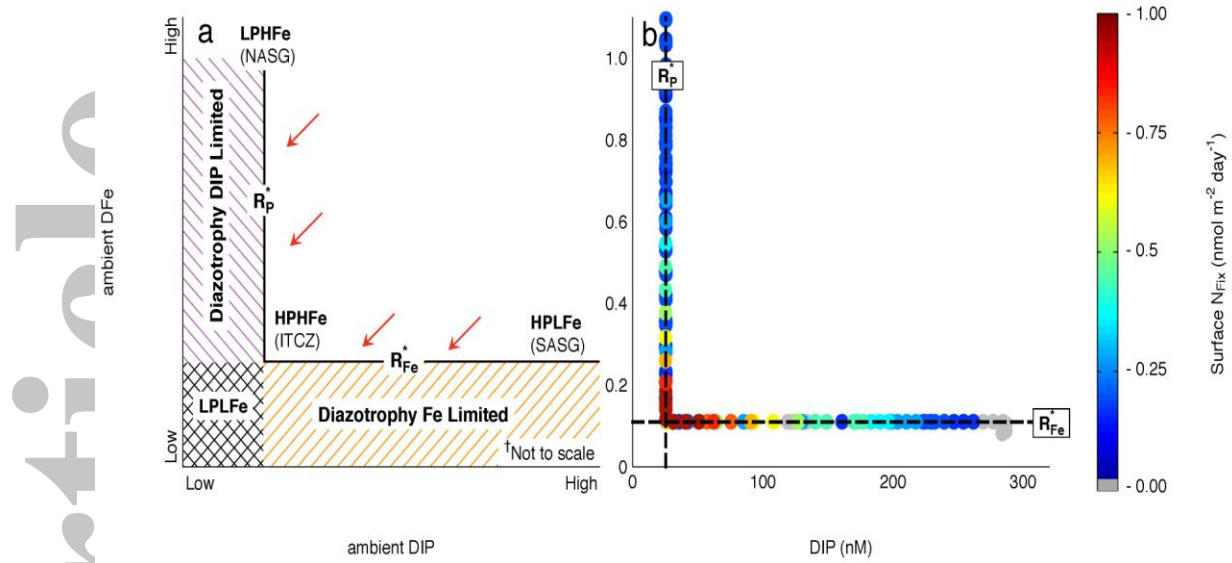


**Figure 8** - A) Graphical representation of the resource competition theory conceptual framework. Red arrows indicate nutrient consumption vectors. B) Numerical model output showing surface N<sub>2</sub> fixation rates (nmol m<sup>-2</sup> d<sup>-1</sup>) as a combined function of DIP (nM) and DFe (nM) for a range of different model realisations.

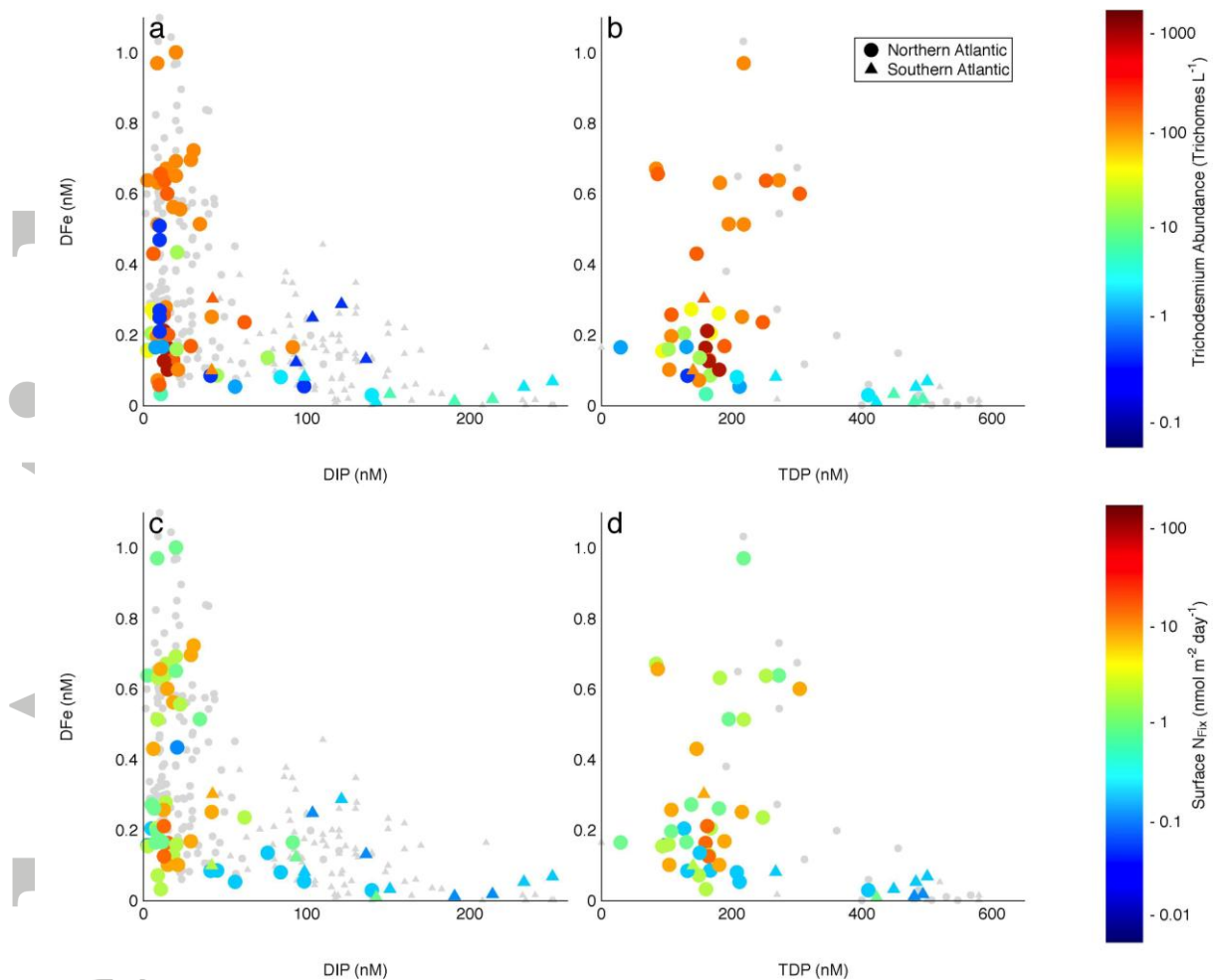


**Figure 9** - Relationship between DIP (nM) and DFe (nM) across the complete data set including stations where no measurements of either *Trichodesmium* abundance or net community N<sub>2</sub> fixation rates were available (grey symbols). Panels A) & B) - *Trichodesmium* abundance (Trichomes L<sup>-1</sup>) as a function of DFe (nM) and either DIP (A) or TDP (B) (nM). Panels C) & D) - Surface N<sub>2</sub> fixation rates (nmol m<sup>-2</sup> d<sup>-1</sup>) as a function of DFe (nM) and either DIP (C) or TDP (D) (nM). Circles denote observations taken from the northern hemisphere whilst triangles denote observations from the southern hemisphere.

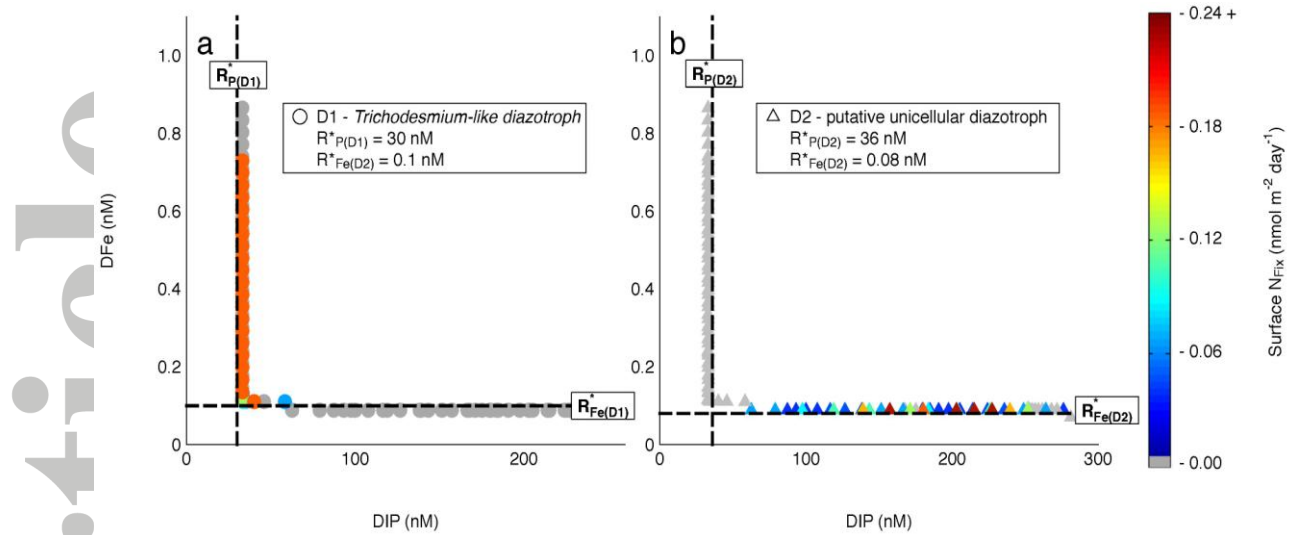


**Figure 10** - Model output showing surface  $N_2$  fixation rates (nmol m<sup>-2</sup> d<sup>-1</sup>) as a function of DIP (nM) and DFe (nM) for two theoretical diazotrophs, D1 a *Trichodesmium*-like diazotroph best at competing for P (A) and D2 a putative-unicellular diazotroph best at competing for Fe (B).